

A vibronic model for the absorption spectra of Cr^{2+} ions in $\text{CdSe}_x\text{S}_{1-x}$

This article has been downloaded from IOPscience. Please scroll down to see the full text article.

2007 J. Phys.: Condens. Matter 19 486213

(<http://iopscience.iop.org/0953-8984/19/48/486213>)

View [the table of contents for this issue](#), or go to the [journal homepage](#) for more

Download details:

IP Address: 129.252.86.83

The article was downloaded on 29/05/2010 at 06:56

Please note that [terms and conditions apply](#).

A vibronic model for the absorption spectra of Cr²⁺ ions in CdSe_xS_{1-x}

Sophia Klokishner¹, Oleg Reu¹, Sergei Ostrovsky¹, Andrew Palii¹ and Elias Towe²

¹ Institute of Applied Physics, Academy of Sciences of Moldova, Academy Street 5, MD-2028, Kishinev, Moldova

² Electronics Engineering Department, Carnegie-Mellon University, Pittsburgh, PA 15213, USA

E-mail: klokishner@yahoo.com

Received 26 September 2007, in final form 17 October 2007

Published 13 November 2007

Online at stacks.iop.org/JPhysCM/19/486213

Abstract

In the present paper we report a vibronic model for the absorption bands of the Cr²⁺ ion in CdSe and CdSe_{0.6}S_{0.4} crystals. For the most probable impurity clusters, CrSe₄, CrSe₃S, CrSeS₃ and CrSe₂S₂, the crystal field splittings and the vibronic coupling parameters are estimated with the aid of the exchange charge model of the crystal field accounting for the exchange and covalence effects. On this basis the transitions responsible for the formation of the optical bands arising from the CrSe₄, CrSe₃S, CrSeS₃ and CrSe₂S₂ species are determined and the profiles of the absorption bands corresponding to these species are calculated. The total spectrum of the CdSe_{0.6}S_{0.4}:Cr²⁺ crystal is obtained by summation over partial spectra arising from all mentioned species. The profiles of the absorption bands in CdSe:Cr²⁺ and CdSe_{0.6}S_{0.4}:Cr²⁺ calculated on the basis of the numerical solution of the dynamical vibronic problems prove to be in quite good agreement with the experimental data.

In memory of Professor Yurii Perlin (17 September 1917–10 March 1990)—to highlight his exceptional achievements and kudos.

1. Introduction

Room-temperature mid-IR (2–5 μm) sources of radiation combining variable spatial coherence with continuous ultrabroad or multiwavelength spectra are of vital importance for many areas of research and technical applications. Since the pioneering research works of Deloach *et al* [1] and Page *et al* [2] on detailed investigation of the spectral properties of metal-doped zinc chalcogenides, laser operation on the ⁵E → ⁵T₂ transition in the Cr²⁺ ion in chalcogenide host materials [3, 4] like ZnSe, CdSe, ZnS and CdMnTe has been demonstrated. Recently an optical study of CdSe_xS_{1-x} crystals doped with Cr²⁺ has been performed [5]. Due to the larger thermal

conductivity of CdS compared to CdSe the CdSeS alloy may be considered as an improvement over the CdSe system. Alloying with CdS gives the possibility of shifting the position of the ${}^5E \rightarrow {}^5T_2$ band in the Cr^{2+} ion towards higher energies and increasing the band gap of the host material, which might decrease the chance of excited state absorption. Thus, recent experimental findings clearly indicate wide prospects for the application of II–VI crystals doped with transition metal ions. At the same time investigations of new materials for IR quantum electronics will be successful if these investigations are supported by theoretical modelling of the spectroscopic and relaxation characteristics of the systems under consideration. The cornerstone in the theoretical consideration of the optical spectra of doped crystals and the lifetimes of excited impurity states is the vibronic coupling of the metal ions with the lattice vibrations. It is this interaction that closely relates to the possibility of tunable lasing on broad phonon assisted bands and the main features of the active media. Although the first fundamental works on the vibronic Jahn–Teller (JT) interactions and optical spectra of the impurity ions in II–VI crystals were performed in the early 1970s the problem of the lifetimes and band shapes for the vibronically assisted transitions is far from being solved and applied for actual lasing materials. In the initial model proposed in [6] the experimental data on Cr-doped II–VI compounds were interpreted in terms of a strong static JT coupling with the vibrational modes of e-symmetry in the ground 5T_2 state. The model suggested in [7] for ZnSe:Cr $^{2+}$ was also based on the assumption that only the e-mode participates in the intra-ion absorption and luminescence transitions. In this paper the quadratic vibronic interaction in the excited 5E state was taken into account. A dynamic JT model was developed in [8]. Further study of II–VI crystals doped with Cr $^{2+}$ ions and other transition metal ions [9, 10] led to essential progress and also demonstrated that the data obtained using different experimental methods could be explained from a common point of view under the assumption of the dynamic JT effect. At the same time the main outcome of the recent papers [10, 11] concerned the structure of the zero-phonon lines of V $^{2+}$ and Cr $^{2+}$ ions in II–VI compounds at low temperatures. In [11] it was found that e-modes only lead to intensities that do not agree well with those of the zero-phonon doublet observed both in emission and absorption in the cases of ZnS and ZnSe, while t_2 modes give a good explanation of transition energies and transition strengths in the same cases. Due to the lack of information regarding the vibronic coupling constants the models developed earlier for transition metal ion (TMI)-doped II–VI compounds were based on the consideration of the interaction of the impurity centre with the only kinds of JT modes (e or t_2), with the subsequent determination of the vibronic coupling constant from the fit to experimental data. Quantum-mechanical calculations of the shapes of the optical bands with allowance for the JT effect in both the initial and final states have not been performed.

A theoretical study of the vibronic JT interaction in a series of II–VI crystals doped with Cr $^{2+}$ ion was reported for the first time in our recent papers [12, 13]. For the tetrahedrally coordinated Cr $^{2+}$ ion (high-spin d^4 configuration) the vibronic coupling parameters were evaluated in the framework of the exchange charge model of the crystal field accounting for the exchange and covalence effects [14–16], and on the basis of these calculations the JT problem was formulated. An examination of the optical absorption bands in CdSe:Cr $^{2+}$ and mixed CdSe $_x$ S $_{1-x}$:Cr $^{2+}$ ($x > 0$) crystals has never been performed. In the present communication we report a model of the absorption bands of the Cr $^{2+}$ ion in CdSe and CdSe $_{0.6}$ S $_{0.4}$. Within the framework of this model for the CdSe $_{0.6}$ S $_{0.4}$:Cr $^{2+}$ system the most probable distributions of selenium and sulfur atoms in the nearest surroundings of Cr $^{2+}$ will be determined. First, for these ligand surroundings of Cr $^{2+}$ the crystal field splittings and the vibronic coupling parameters will be microscopically calculated. Then, the subsequent evaluation of the profiles of the optical absorption bands in CdSe:Cr $^{2+}$ and mixed CdSe $_{0.6}$ S $_{0.4}$:Cr $^{2+}$ crystals will be performed.

2. Possible arrangements of selenium and sulfur atoms in the nearest surroundings of cadmium

The observed shift of the ${}^5E \rightarrow {}^5T_2$ band position in the $\text{CdSe}_{0.6}\text{S}_{0.4}$ crystal can be attributed to the formation of impurity complexes with different contents of sulfur and selenium atoms in the nearest surroundings of the Cr^{2+} ion. As the first step we examine a pure $\text{CdSe}_{0.6}\text{S}_{0.4}$ crystal and calculate the number of complexes in which the Cd^{2+} ions are surrounded by: (i) four selenium atoms; (ii) three selenium atoms and one sulfur atom; (iii) two selenium atoms and two sulfur atoms; (iv) three sulfur atoms and one selenium atom; (v) four sulfur atoms. The probability of existence of a certain tetrahedral surrounding is given by the expression

$$P_i = C_m^n P_{\text{Se}}^n P_{\text{S}}^m, \quad (1)$$

where P_{Se} and P_{S} are the fractional concentrations of Se and S atoms, respectively, i.e. the probabilities that the given neighbour of the Cd^{2+} ion is a selenium or a sulfur atom, $C_m^n = n!/(m!(n-m)!)$ is the binomial coefficient that describes the number of possible combinations for m objects to be placed in n sites ($m \leq n$), n and m are the numbers of Se and S atoms in the considered neighbourhood configuration, respectively. Then, for the fractional concentrations $P_{\text{Se}} = 0.6$ and $P_{\text{S}} = 0.4$, one can easily calculate the probabilities of existence of all mentioned distributions:

$$P_1 = C_0^4 P_{\text{Se}}^4 = 0.1296; \quad P_2 = C_1^4 P_{\text{Se}}^3 P_{\text{S}} = 0.3456; \quad P_3 = C_3^4 P_{\text{Se}} P_{\text{S}}^3 = 0.1536; \quad (2)$$

$$P_4 = C_2^4 P_{\text{Se}}^2 P_{\text{S}}^2 = 0.3456 \quad P_5 = C_4^4 P_{\text{S}}^4 = 0.0256.$$

From equation (2) it follows that the second and fourth configurations are the most probable ones; at the same time the first and third configurations are less frequent, but also give an appreciable contribution. Finally, the fifth configuration has a negligible probability and will be neglected in all subsequent calculations. We assume that the Cr^{2+} ions are distributed randomly in the $\text{CdSe}_{0.6}\text{S}_{0.4}$ lattice and substitute the Cd^{2+} ones in different mixed surroundings of sulfur and selenium with equal probability. Under such an assumption the number of impurity clusters CrSe_4 , CrSe_3S , CrSe_2S_2 and CrS_3Se prove to be proportional to P_1 , P_2 , P_3 and P_4 , respectively. The total absorption spectra of the $\text{CdSe}_{0.6}\text{S}_{0.4}:\text{Cr}^{2+}$ system will be calculated as a sum of spectra arising from CrSe_4 , CrSe_2S_2 , CrSe_3S and CrS_3Se species. Each particular contribution in this sum will be multiplied by the corresponding statistical weight given by equation (2).

3. The Hamiltonian of the system

The total Hamiltonian for the impurity ion in a crystal can be represented as

$$H = H_e(\mathbf{r}, \mathbf{R}_0) + H_v(q) + H_{ev}(\mathbf{r}, q), \quad (3)$$

where \mathbf{r} and q are the sets of the electronic and vibrational coordinates, respectively. $H_e(\mathbf{r}, \mathbf{R}_0)$ is the electronic Hamiltonian determining the wavefunctions and the eigenvalues of the impurity ion in a fixed nuclear configuration $q = 0$. This configuration corresponds to the positions of the ions $\mathbf{R} = \mathbf{R}_0$ in the host lattice and does not take into account the lattice relaxation arising from the embedding of the ion in the ground state. $H_v(q)$ is the Hamiltonian of the free lattice vibrations:

$$H_v = \sum_{\bar{\mu}\bar{\Gamma}\bar{\gamma}} \frac{\hbar\omega_{\bar{\mu}\bar{\Gamma}}}{2} \left(q_{\bar{\mu}\bar{\Gamma}\bar{\gamma}}^2 - \frac{\partial^2}{\partial q_{\bar{\mu}\bar{\Gamma}\bar{\gamma}}^2} \right), \quad (4)$$

where $q_{\bar{\mu}\bar{\Gamma}\bar{\gamma}}$ are the symmetry adapted vibrational coordinates corresponding to the irreducible representations (irreps) $\bar{\Gamma}$ (including multiple representations) and $\omega_{\bar{\mu}\bar{\Gamma}}$ is the frequency of the

vibration $\bar{\mu}\bar{\Gamma}$ (symbol $\bar{\mu}$ enumerates the repeating vibrational representations). Denoting the displacements of the ions of the impurity complex from their positions \mathbf{R}_p^0 (at $q = 0$) by $\Delta\mathbf{R}_p = \mathbf{R}_p - \mathbf{R}_p^0$ (p is the index of the position) these vibration coordinates can be written as:

$$q_{\bar{\mu}\bar{\Gamma}\bar{\gamma}} = \frac{1}{l_{\bar{\Gamma}}} \sum_p U_p^{\bar{\mu}\bar{\Gamma}\bar{\gamma}} \Delta\mathbf{R}_p, \quad (5)$$

where $U_{p\alpha}^{\bar{\mu}\bar{\Gamma}\bar{\gamma}}$ ($\alpha = x, y, z$) are the elements of the unitary matrix for the transformation of the Cartesian displacements $\Delta\mathbf{R}_p$ into the dimensionless coordinates $q_{\bar{\mu}\bar{\Gamma}\bar{\gamma}}, l_{\bar{\mu}\bar{\Gamma}} = (\hbar\omega_{\bar{\mu}\bar{\Gamma}}/f_{\bar{\mu}\bar{\Gamma}})^{1/2}$ and $f_{\bar{\mu}\bar{\Gamma}}$ is the force constant corresponding to this vibration. Finally, the last part of the Hamiltonian (3) is the vibronic interaction for the impurity ion (related also to the positions $\mathbf{R} = \mathbf{R}_0$). The operator H_{ev} consists of the parts corresponding to the vibrational irreps of the impurity cluster of the defined symmetry:

$$H_{ev} = \sum_{\bar{\mu}\bar{\Gamma}\bar{\gamma}} v_{\bar{\mu}\bar{\Gamma}\bar{\gamma}}(\mathbf{r}) q_{\bar{\mu}\bar{\Gamma}\bar{\gamma}}. \quad (6)$$

The operator $v_{\bar{\mu}\bar{\Gamma}\bar{\gamma}}(\mathbf{r})$ with the dimension of energy can be expressed as:

$$v_{\bar{\mu}\bar{\Gamma}\bar{\gamma}}(\mathbf{r}) = \sum_{p,i} \left. \frac{\partial W(\mathbf{r}_i - \mathbf{R}_p)}{\partial q_{\bar{\mu}\bar{\Gamma}\bar{\gamma}}} \right|_{q_{\bar{\mu}\bar{\Gamma}\bar{\gamma}}=0} = l_{\bar{\mu}\bar{\Gamma}} \sum_{p,i} \left. \frac{\partial W(\mathbf{r}_i - \mathbf{R}_p)}{\partial \mathbf{R}_p} \right|_{\mathbf{R}_p=\mathbf{R}_p^0} \times U_p^{\bar{\mu}\bar{\Gamma}\bar{\gamma}} = \sum_i v_{\bar{\mu}\bar{\Gamma}\bar{\gamma}}(\mathbf{r}_i), \quad (7)$$

where $W(\mathbf{r}_i - \mathbf{R}_p)$ is the potential energy of the interaction between the i th electron of the ion and the p th atom of the host crystal in the position \mathbf{R}_p^0 .

The next step of our consideration is the derivation of the symmetry adapted vibrational coordinates $q_{\bar{\mu}\bar{\Gamma}\bar{\gamma}}$ and operators $v_{\bar{\mu}\bar{\Gamma}\bar{\gamma}}(\mathbf{r})$ of electron-vibrational interaction for the impurity complexes CrSe₄, CrSe₃S, CrSe₂S₂ and CrS₃Se. We assume that the replacement of selenium atoms by sulfur ones does not displace the position of the Cr²⁺ ion in the mentioned complexes and leads only to the change of the symmetry of the immediate environment due to the different radii of Se and S atoms. It is supposed that in the complexes CrSe₄ and CrSe₂S₂ the symmetry of the ligand field is T_d and C_{2v} (figures 1(a) and (b)), respectively, while in the complexes CrSe₃S and CrS₃Se the Cr ions acquire a trigonal symmetry surrounding (C_{3v}) (figures 1(c) and (d)). In the case of a tetrahedral complex CrSe₄ we are dealing with the full symmetric A₁ tetragonal E and two trigonal vibrations, T₂⁽¹⁾ and T₂⁽²⁾. For this complex the symmetry adopted coordinates $q_{\bar{\mu}\bar{\Gamma}\bar{\gamma}}$ and the operators $v_{\bar{\mu}\bar{\Gamma}\bar{\gamma}}(\mathbf{r})$ obtained in the exchange charge model of the crystal field [12–16] are given in [13]. For the complex CrSe₃S of C_{3v} symmetry the active vibrations are two full symmetric vibrations A₁⁽¹⁾, A₁⁽²⁾ and two doubly degenerate vibrations E⁽¹⁾ and E⁽²⁾. The corresponding symmetrized displacements $q_{\bar{\mu}\bar{\Gamma}\bar{\gamma}}$ are given in the appendix. In the case when the local Cr²⁺ surroundings consist of three S and one Se atom the symmetry adopted coordinates $q_{\bar{\mu}\bar{\Gamma}\bar{\gamma}}$ are also expressed by relations (A.1) with the single difference that now the mass m corresponds to the sulfur atom while the selenium atom possesses the mass M . The low-symmetry complex C_{2v} only possesses one-dimensional vibrations: three full symmetric vibrations A₁⁽¹⁾, A₁⁽²⁾, A₁⁽³⁾ and three nonsymmetric vibrations A₂, B₁ and B₂. The vibrational coordinates $q_{\bar{\mu}\bar{\Gamma}\bar{\gamma}}$ for this complex are also given in the appendix.

4. Absorption band of the CrSe₄ complex

The ground ⁵D term of a free Cr²⁺ ion (high-spin electronic configuration d⁴) is split by the tetrahedral crystal field in a CrSe₄ species into the orbital triplet ⁵T₂(t₂²e²) and orbital doublet

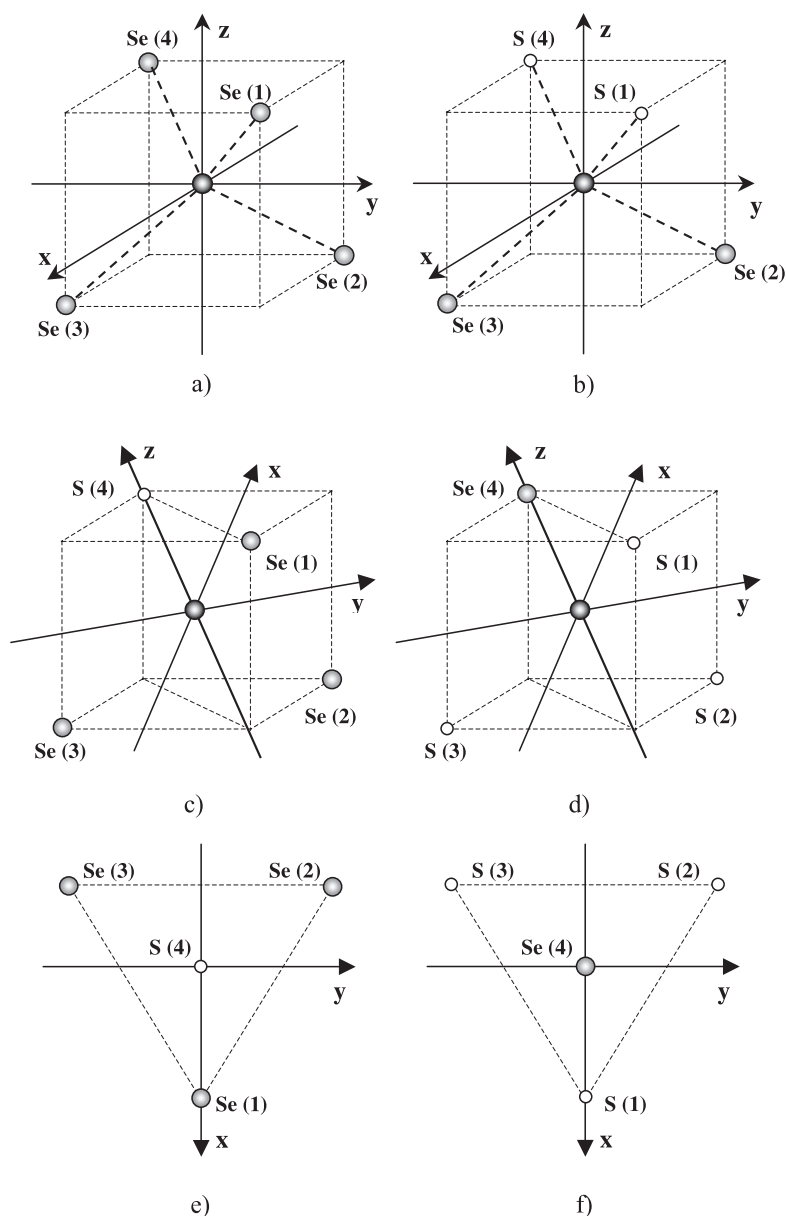


Figure 1. Ligand arrangements in the $\text{CrSe}_{4-y}\text{S}_y$ ($y = 0-3$) clusters with the indication of corresponding frames of reference: (a) CrSe_4 ; (b) CrSe_2S_2 ; (c) CrSe_3S ; (d) CrSeS_3 ; top view of CrSe_3S (e) and CrSeS_3 (f) species.

$^5\text{E}(t_2^3e)$, the former being the ground term (figure 2(a)). In the strong crystal field basis the determinant wavefunctions $|t_2^n(S_1\Gamma_1)e^m(S_2\Gamma_2)S\Gamma\gamma M_S\rangle$ for these two terms $S\Gamma$ of Cr^{2+} ion are given by:

$$\begin{aligned}
 |t_2^3(^4A_2)e(^2E)^5Eu, M_S = 2\rangle &= |\xi\eta\zeta\nu\rangle, & |t_2^2(^3T_1)e(^3A_2)^5T_2\zeta, \\
 M_S = 2\rangle &= |\xi\eta u\nu\rangle, &
 \end{aligned}
 \tag{8}$$

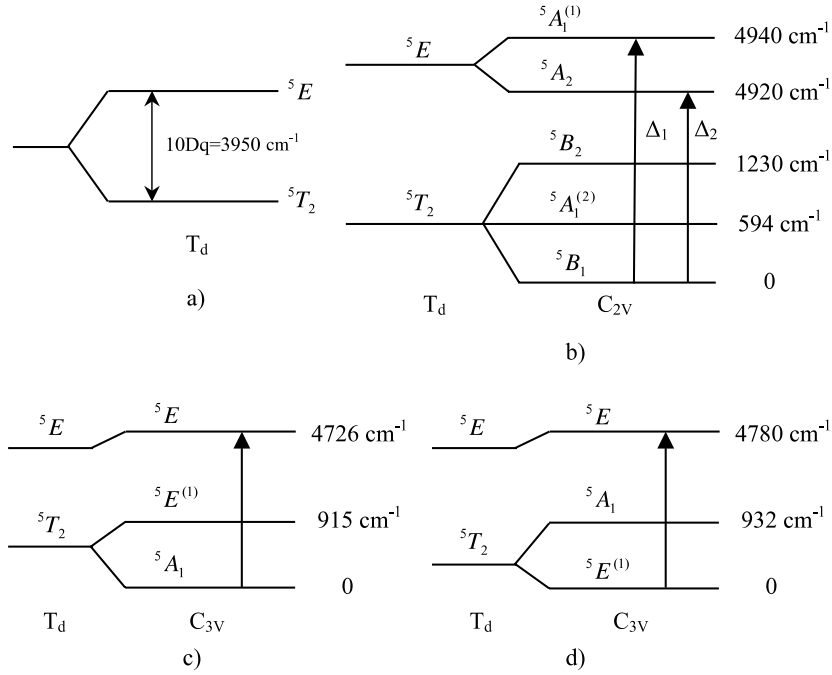


Figure 2. Crystal field splittings for the impurity $\text{CrSe}_{4-y}\text{S}_y$ ($y = 0-3$) clusters: (a) CrSe_4 ; (b) CrSe_2S_2 ; (c) CrSe_3S ; (d) CrSeS_3 .

where the symbol γ enumerates the basis functions of the irrep Γ (E and T_2), M_S is the spin projection and the conventional notation $|\dots\rangle$ is used for the Slater determinants. The standard cubic basis sets for the one-electron d -functions $T_2(\xi, \eta, \zeta)$ ($\xi \propto yz, \eta \propto xz, \zeta \propto xy$) and $E(u, v)$ ($u \propto 3z^2 - r^2, v \propto \sqrt{3}(x^2 - y^2)$) are used. In equation (8) the only wavefunction for each degenerate term is given; the basis is related to the C_2 axis of the tetrahedron.

First, we present the Hamiltonian (3) of the system in the form [12, 13]

$$H = H_0 + H', \quad (9)$$

where

$$H_0 = H_e(\mathbf{r}, \mathbf{R}_0) + \nu_{A_1}(\mathbf{r})q_0 + \frac{\hbar\omega_{A_1}}{2}q_0^2 + \frac{\hbar\omega_{A_1}}{2}\left(Q^2 - \frac{\partial^2}{\partial Q^2}\right) + \sum_{\mu_1\bar{\Gamma}\bar{\gamma}} \frac{\hbar\omega_{\mu_1\bar{\Gamma}}}{2}\left(q_{\mu_1\bar{\Gamma}\bar{\gamma}}^2 - \frac{\partial^2}{\partial q_{\mu_1\bar{\Gamma}\bar{\gamma}}^2}\right) \quad (10)$$

$$H' = \nu_{A_1}(\mathbf{r})Q + \sum_{\mu_1\bar{\Gamma}\bar{\gamma}} \nu_{\mu_1\bar{\Gamma}\bar{\gamma}}(\mathbf{r})q_{\mu_1\bar{\Gamma}\bar{\gamma}} \quad (11)$$

$Q = q_{A_1} - q_0$ is the full symmetric coordinate counted off from the new equilibrium position

$$q_0 = -V_{T_2}/\hbar\omega_{A_1}, \quad \langle {}^5T_2(t_2^2e^2) | \nu_{A_1}(\mathbf{r}) | {}^5T_2(t_2^2e^2) \rangle = V_{T_2} \quad \text{and} \quad (12)$$

$$\nu_{A_1}(\mathbf{r}) = \mathbf{v}_{A_1}(\mathbf{r}) + \hbar\omega_{A_1}q_0$$

is the redefined vibronic operator for full symmetric A_1 vibrations adapted to the new positions of the ions, the index μ_1 stands for tetragonal E and trigonal $T_2^{(1)}, T_2^{(2)}$ vibrational modes of the tetrahedral complex.

One can easily prove that

$$\langle {}^5T_2 | \nu_{A_1}(\mathbf{r}) | {}^5T_2 \rangle \equiv \nu_{A_1}(T_2) = 0, \quad \langle {}^5E | \nu_{A_1}(\mathbf{r}) | {}^5E \rangle \equiv \nu_{A_1}(E) = \nu_t - \nu_e, \quad (13)$$

where ν_t and ν_e are the single electron matrix elements. The vibronic Hamiltonian for the ${}^5T_2 \otimes (e + 2t_2)$ JT problem is the following:

$$H_{ev}(T_2) = \nu_E(T_2)(O_{Eu}q_{Eu} + O_{Ev}q_{Ev}) + \nu_{T_2}^{(1)}(T_2)(O_{T_2\xi}q_{T_2\xi}^{(1)} + O_{T_2\eta}q_{T_2\eta}^{(1)} + O_{T_2\zeta}q_{T_2\zeta}^{(1)}) \\ + \nu_{T_2}^{(2)}(T_2)(O_{T_2\xi}q_{T_2\xi}^{(2)} + O_{T_2\eta}q_{T_2\eta}^{(2)} + O_{T_2\zeta}q_{T_2\zeta}^{(2)}). \quad (14)$$

For the ${}^5E \otimes (a_1 + e)$ problem one finds

$$H_{ev}(E) = \nu_E(E)(O'_{Eu}q_{Eu} + O'_{Ev}q_{Ev}) + \nu_{A_1}(E)O_{A_1}Q. \quad (15)$$

All matrices in equations (14) and (15) are defined through the Clebsch–Gordan coefficients: $\langle \Gamma\gamma | O_{\bar{\Gamma}\bar{\gamma}} | \Gamma\gamma' \rangle = \langle \Gamma\gamma | \Gamma\gamma' \bar{\Gamma}\bar{\gamma} \rangle$ for the T_d point symmetry group. In equations (14) and (15) the values $\nu_{\bar{\Gamma}}^{\mu}(\Gamma) = [\Gamma]^{-1/2} \langle \Gamma \parallel \nu_{\mu\bar{\Gamma}} \parallel \Gamma \rangle$ ($[\Gamma]$ is the dimension of the irrep Γ) are the vibronic coupling constants for the vibrations $T_2^{(1)}$, $T_2^{(2)}$ and E , $\langle \Gamma \parallel \nu_{\mu\bar{\Gamma}} \parallel \Gamma \rangle$ is the reduced matrix element of the operator $\nu_{\mu\bar{\Gamma}}(\mathbf{r})$, while $\nu_{A_1}(E) = \langle E \parallel \nu_{A_1} \parallel E \rangle / \sqrt{2} - \langle T_2 \parallel \nu_{A_1} \parallel T_2 \rangle / \sqrt{3}$. The ground ${}^5T_2(t_2^2e^2)$ and excited ${}^5E(t_2^3e)$ terms of the Cr^{2+} ion are orbitally degenerate, resulting in $T_2 \otimes (a_1 + e + 2t_2)$ and $E \otimes (a_1 + e)$ JT vibronic problems. In the exchange charge model of the crystal field [14–16] the expressions for the vibronic coupling constants are as follows:

$$\nu_{A_1}(E) = -\frac{2e^2 l_{A_1}}{27R^6} (25Z \langle r^4 \rangle + 18R^4 G(S_4(R) - RS'_4(R))), \\ \nu_E(E) = -\frac{8e^2 l_E}{63R^6} (5Z \langle r^4 \rangle - 9Z \langle r^2 \rangle R^2 - 18R^4 G S_2(R) + 18R^4 G S_4(R)), \\ \nu_E(T_2) = \frac{4\sqrt{2}e^2 l_E}{189R^6} (20Z \langle r^4 \rangle + 27Z \langle r^2 \rangle R^2 + 54R^4 G S_2(R) + 72R^4 G S_4(R)), \\ \nu_{T_2}^{(1)}(T_2) = \frac{2\sqrt{2}e^2 l_{T_2}^{(1)}}{189R^6} ((100 \langle r^4 \rangle + 81 \langle r^2 \rangle R^2)Z - 18GR^4(-3S_2(R) - 4S_4(R)) \\ + 3RS'_2(R) + 4RS'_4(R)) \\ \nu_{T_2}^{(2)}(T_2) = \frac{4e^2 l_{T_2}^{(2)}}{189R^6} ((27R^2 \langle r^2 \rangle - 50 \langle r^4 \rangle)Z + 18GR^4(3S_2(R) - 10S_4(R))) \quad (16)$$

where $l_{\bar{\Gamma}} = (\hbar\omega_{\bar{\Gamma}}/f_{\bar{\Gamma}})^{1/2}$, $\omega_{\mu\bar{\Gamma}}$ is the frequency of the vibration $\bar{\Gamma}$ and $f_{\bar{\Gamma}}$ is the force constant, R is the distance between the Cr^{2+} ion and the ligands, $S_2(R)$, $S_4(R)$ are the overlap integrals [12, 13]:

$$S_l(R) = S_s^2(R) + S_\sigma^2(R) + \gamma_l S_\pi^2(R), \quad \gamma_2 = 1, \quad \gamma_4 = -4/3, \\ S_s(R) = \langle 3d, m = 0 | n''s \rangle, \quad S_\sigma(R) = \langle 3d, m = 0 | n''p, m = 0 \rangle, \\ S_\pi(R) = \langle 3d, m = \pm 1 | n''p, m = \pm 1 \rangle,$$

$|3dm\rangle$ and $|n''s\rangle$, $|n''pm\rangle$ are the Cr^{2+} and the ligands wavefunctions, respectively, $S'_l(R) = \frac{dS_l(R)}{dR}$. In all subsequent calculations we employ the simplest version of the exchange charge model with the only phenomenological dimensionless parameter G that has been determined with the aid of the relation

$$Dq = -\frac{2(5Ze^2 \langle r^4 \rangle + 18R^4 G S_4(R))}{135R^5} \quad (17)$$

and shown to be equal in $CdSe:Cr^{2+}$ and $CdS:Cr^{2+}$ crystals (see table 1). The overlap integrals $S_2(R)$, $S_4(R)$ have been computed using the radial atomic ‘double zeta’ 3d wavefunctions of

Table 1. Parameters of the exchange charge model for CdSe and CdS crystals doped with Cr²⁺ ions (a_0 is the Bohr radius).

Crystal	Dq (cm ⁻¹)	G	R (Å)	$S_2(R)$	$S_4(R)$	$S'_2(R)$ (a_0^{-1})	$S'_4(R)$ (a_0^{-1})	$\hbar\omega$ (cm ⁻¹)	Z
CdS	-465	2.71	2.52	0.0163	0.0102	-0.0212	-0.0102	80	2
CdSe	-395	2.71	2.62	0.0149	0.0091	-0.0180	-0.008	60	2

Table 2. Vibronic coupling constants (in cm⁻¹) for the CrSe₄ complex.

$\nu_E(T_2)$			$\nu_{T_2}^{(1)}(T_2)$			$\nu_{T_2}^{(2)}(T_2)$			$\nu_{A_1}(E)$			$\nu_E(E)$		
pc	ec	Total	pc	ec	Total	pc	ec	Total	pc	ec	Total	pc	ec	Total
66	49	115	106	154	260	27	-20	7	-24	-74	-98	73	15	88

chromium, 4s, 4p functions of selenium and 3s, 3p functions of sulfur given in [17]. It should be mentioned that for species CrSe_{4-y}S_y ($y = 1-3$) with mixed ligand surroundings the energy levels and vibronic coupling constants are determined through overlap integrals $S_j(R_i)$ and their derivatives $S'_j(R_i) = \frac{dS_j(R_i)}{dR_i}$, where $R_i = R, R_0, R$ and R_0 are the distances between the Cr²⁺ ion and Se and S atoms, respectively. The evaluated overlap integrals and their derivatives as well as the parameters used for calculations of the vibronic coupling constants are collected in table 1. The calculated vibronic coupling constants for all active modes of the CrSe₄ complex are given in table 2. Each vibronic constant is presented as a sum of contributions arising from the electrostatic field of point ligand charges and from the exchange charge field, the last can be considered as a measure of the effect of covalence. It is seen that the main contribution to the vibronic coupling constants $\nu_E(T_2)$, $\nu_{T_2}^{(1)}(T_2)$, $\nu_E(E)$ in most cases comes from the field of point charges. Meanwhile, the exchange charge field yields a dominant contribution to the vibronic parameters $\nu_{T_2}^{(1)}(T_2)$ and $\nu_{A_1}(E)$. The data listed in table 2 also show that for the ⁵E term the interaction with the E and A₁ modes is approximately of the same strength. The JT interaction with the T₂⁽¹⁾ vibrations proves to be dominant within the ⁵T₂ term. The interaction of this term with the E-mode is more than two times weaker than that with the T₂⁽¹⁾ vibrations. At the same time the interaction with the second vibration of T₂ symmetry is negligible for this term. The results obtained from the calculation of the vibronic coupling constants have been used for the description of the observed absorption band arising on the transition ⁵T₂ → ⁵E of the CrSe₄ cluster. Taking into account the predominant role of the interaction of the ground ⁵T₂ term with the trigonal T₂⁽¹⁾ vibrations at the first step in the evaluation of the shape of the absorption ⁵T₂ → ⁵E band we will consider three-mode JT problems (e + a₁) ⊗ E for the ⁵E state and t₂ ⊗ T₂ for the ⁵T₂ state. It should also be noted that for the Cr²⁺ ion the spin-orbital interaction (the constant of this interaction $\lambda = 57$ cm⁻¹ [6]) is much weaker than the interaction with the T₂⁽¹⁾ vibrations of the CrSe₄ complex. At the same time the effects of spin-orbital interaction, such as the splitting of the zero-phonon lines, are observed at very low temperatures. Taking into account both these factors in the calculation of the shape of the ⁵T₂ → ⁵E band at room temperature the effect of spin-orbital interaction was not considered.

The ground ⁵T₂ term is well isolated from the excited ones so that the hybrid vibronic states corresponding to the dynamical JT problem in this state can be expressed as an expansion in terms of the products of zeroth-order approximation electronic functions and the harmonic oscillator functions for the full symmetric, tetragonal and trigonal vibrations

$$\psi_{n_1, n_u, n_v}^{(v)} = \Phi_{n_1}(Q) \Phi_{n_u}(q_u) \Phi_{n_v}(q_v) \sum_{\substack{\gamma=\xi, \eta, \zeta \\ n_\xi, n_\eta, n_\zeta}} C_{\gamma, n_\xi, n_\eta, n_\zeta}^{(v)} \Phi_{n_\xi}(q_\xi) \Phi_{n_\eta}(q_\eta) \Phi_{n_\zeta}(q_\zeta) |\gamma\rangle, \quad (18)$$

where the symbol ν enumerates the hybrid (electron–vibrational) states, $n_1 \equiv n_{A_1}$, $|\gamma\rangle$ stands for the electronic wavefunctions ξ, η, ζ of the 5T_2 state, $\Phi_{n_1}(Q)$, $\Phi_{n_u}(q_u)$, $\Phi_{n_v}(q_v)$, $\Phi_{n_\xi}(q_\xi)$, $\Phi_{n_\eta}(q_\eta)$, $\Phi_{n_\zeta}(q_\zeta)$ denote the harmonic oscillator wavefunctions corresponding to the A_1, E and $T_2^{(1)}$ vibrations, respectively; actually the coefficients $C_{n_\xi, n_\eta, n_\zeta}^{(\nu)}$ form the eigenvectors of the infinite JT matrix. The energies of the vibronic levels arising from the $t_2 \otimes T_2$ problem can be presented as

$$E_{n_1, n_u, n_v}^{(\nu)} = \hbar\omega(n_u + n_v + 1) + \hbar\omega(n_1 + 1/2) + \varepsilon_{T_2}^{(\nu)}, \quad (19)$$

where the values $\varepsilon_{T_2}^{(\nu)}$ will be determined from the solution of the $t_2 \otimes T_2$ JT problem for the 5T_2 -term. For the excited 5E state the vibronic wavefunction looks as follows

$$\psi_{n'_1, n_\xi, n_\eta, n_\zeta}^{(\nu')} = \Phi_{n'_1}(Q - Q^0) \Phi_{n_\xi}(q_\xi) \Phi_{n_\eta}(q_\eta) \Phi_{n_\zeta}(q_\zeta) \sum_{\substack{\gamma'=u, v \\ n_u, n_v}} C_{\gamma', n_u, n_v}^{(\nu')} \Phi_{n_u}(q_u) \Phi_{n_v}(q_v) |\gamma'\rangle, \quad (20)$$

where $Q^0 = -v_{A_1}(E)/\hbar\omega$, $\gamma' = u, v$; the sense of other notations is the same as in equation (18). For the 5E term the linear interaction with the full symmetric vibration results in the adiabatic problem, giving rise to a shift Q^0 of the equilibrium position of the Q -coordinate. The corresponding to (20) energy levels can be presented as

$$E_{n'_1, n_\xi, n_\eta, n_\zeta}^{(\nu')} = 10Dq - \frac{(v_{A_1}(E))^2}{2\hbar\omega} + \hbar\omega(n'_1 + 1/2) + \hbar\omega(n_\xi + n_\eta + n_\zeta + 3/2) + \varepsilon_E^{(\nu')}, \quad (21)$$

where energies $\varepsilon_E^{(\nu')}$ will be obtained from the solution of the $e \otimes E$ vibronic problem.

In numerical calculations of the eigenvalues and eigenvectors of the dynamic vibronic problems $e \otimes E$ and $t_2 \otimes T_2$ the vibronic matrices were truncated. For the $e \otimes E$ problem the number N of unperturbed vibrational states satisfied the condition $(n_u + n_v \leq N)$, where in the calculation $N = 100$ was taken. For the $t_2 \otimes T_2$ problem the inequality $n_\xi + n_\eta + n_\zeta \leq 60$ held. The general dimension of the vibronic matrix for the E term was 10302×10302 . For the T_2 term the dimension of the matrix was 119133×119133 . The Lanczos recursion procedure with a proper choice of the initial state was used to calculate the vibronic functions and energies [18].

The shape $F_1(\Omega)$ of the absorption band can be presented as

$$F_1(\Omega) = \frac{1}{Z} \sum_{\substack{v, v' \\ n_\xi, n_\eta, n_\zeta \\ n_1, n'_1, n_u, n_v}} \text{Exp} \left[-\frac{E_{n_1, n_u, n_v}^{(v)}}{kT} \right] \left| \overline{\left\langle \psi_{n'_1, n_\xi, n_\eta, n_\zeta}^{(v')} \middle| \vec{u} \vec{d} \middle| \psi_{n_1, n_u, n_v}^{(v)} \right\rangle} \right|^2 \times \delta(E_{n'_1, n_\xi, n_\eta, n_\zeta}^{(v')} - E_{n_1, n_u, n_v}^{(v)} - \hbar\Omega), \quad (22)$$

where \vec{d} and \vec{u} are the dipole moment and polarization vectors, respectively, the symbol $\overline{|\dots|^2}$ means the averaging over the light polarization,

$$Z = \sum_{\substack{v, \\ n_1, n_u, n_v}} \text{Exp} \left[-\frac{E_{n_1, n_u, n_v}^{(v)}}{kT} \right] = \sum_v \text{Exp} \left(-\frac{\varepsilon_{T_2}^{(v)}}{kT} \right) / 8 \sinh^3(\beta/2)$$

is the partition function for the ground states, equation (22) contains averaging over the initial states (n_1, n_u, n_v, v) and summation over the final $(n'_1, n_\xi, n_\eta, n_\zeta, v')$ ones, $\beta = \hbar\omega/kT$, hereunder the frequencies of the full symmetric, tetragonal and trigonal vibrations are taken to be equal. The averaging and summation over the states of the A_1 oscillator can be performed

in the conventional way [19] and leads to a well known spectral distribution referred to as ‘Pekarian’. After some transformations equation (22) can be written as

$$F_1(\Omega) = \frac{|\langle {}^5E \parallel d_{T_1} \parallel {}^5T_2 \rangle|^2}{3Z_1} \sum_{\substack{v, v' \\ n_\xi, n_\eta, n_\zeta \\ n_u, n_v}} \text{Exp} \left[-\frac{E_{n_u, n_v}^{(v)}}{kT} \right] \text{Exp} \left[-\frac{1}{2} a \coth \left(\frac{\beta}{2} \right) \right] \\ \times \sum_{n=-\infty}^{\infty} I_n \left(\frac{a}{2 \sinh(\beta/2)} \right) \text{Exp} \left[\frac{n\beta}{2} \right] \left\{ \frac{1}{12} (C_{\xi, n_\xi, n_\eta, n_\zeta}^{(v)})^2 (\sqrt{3} C_{u, n_u, n_v}^{(v')})^2 \right. \\ + C_{v, n_u, n_v}^{(v')} \left. \right)^2 + \frac{1}{12} (C_{\eta, n_\xi, n_\eta, n_\zeta}^{(v)})^2 (\sqrt{3} C_{u, n_u, n_v}^{(v')} - C_{v, n_u, n_v}^{(v')})^2 \\ + \frac{1}{3} \left(C_{\zeta, n_\xi, n_\eta, n_\zeta}^{(v)} \right)^2 (C_{v, n_u, n_v}^{(v')})^2 \left. \right\} \delta(E_{n_\xi, n_\eta, n_\zeta}^{(v')} - E_{n_u, n_v}^{(v)}) \\ + \hbar\omega n - (v_{A_1}(\text{E}))^2 / (2\hbar\omega) - \hbar\Omega \quad (23)$$

$$Z_1 = \sum_v \text{Exp} \left(-\frac{\varepsilon_{T_2}^{(v)}}{kT} \right) / 4 \sinh^2(\beta/2), \quad a = \left(\frac{v_{A_1}(\text{E})}{\hbar\omega} \right)^2,$$

$$E_{n_1, n_u, n_v}^{(v)} - E_{n_u, n_v}^{(v)} = \hbar\omega(n_1 + 1/2), \quad E_{n'_1, n_\xi, n_\eta, n_\zeta}^{(v')} - E_{n_\xi, n_\eta, n_\zeta}^{(v')} = \hbar\omega(n'_1 + 1/2), \quad (24)$$

where $\beta = \hbar\omega/kT$, $I_n(\frac{a}{2 \sinh(\beta/2)})$ is the modified Bessel function and a is the heat release parameter (the Pekar–Huang–Rhys parameter) and $\langle {}^5E \parallel d_{T_1} \parallel {}^5T_2 \rangle$ is the reduced matrix element of the transition dipole moment. From equation (23) it is seen that the resultant optical band is represented by the convolution of two discrete distributions: one is the optical band arising from the JT interaction solely (transitions $n_u, n_v, v \rightarrow$ and $n_\xi, n_\eta, n_\zeta, v'$) and another one is the Pekarian [19] with the heat release parameter a formed by the $n_1 \rightarrow n'_1$ transitions

$$P(10Dq + \hbar\omega n - (v_{A_1}(\text{E}))^2 / 2\hbar\omega) - \hbar\Omega = \text{Exp} \left[-\frac{1}{2} a \coth \left(\frac{\beta}{2} \right) \right] \sum_{n=-\infty}^{\infty} I_n \left(\frac{a}{2 \sinh(\beta/2)} \right) \\ \times \text{Exp} \left[\frac{n\beta}{2} \right] \delta(10Dq + \hbar\omega n - (v_{A_1}(\text{E}))^2 / 2\hbar\omega) - \hbar\Omega). \quad (25)$$

In order to get the envelope curve (that appears due to the dispersion of the lattice vibrations) the shape function of the individual line related to the transition between hybrid vibronic states (n_1, n_u, n_v, v) and $(n'_1, n_\xi, n_\eta, n_\zeta, v')$ is assumed to be of the Gaussian form

$$\frac{1}{\sqrt{2\pi\lambda^2}} \text{Exp} \left[-\frac{(E_{n_\xi, n_\eta, n_\zeta}^{(v')} - E_{n_u, n_v}^{(v)} + \hbar\omega n - (v_{A_1}(\text{E}))^2 / 2\hbar\omega - \hbar\Omega)^2}{2\lambda^2} \right]. \quad (26)$$

To smooth the quantum discrete structure of the calculated band the second central moment of the individual lines λ should be comparable with the $\hbar\omega$ value. In further calculations for the CrSe₄ moiety we put $\lambda = \hbar\omega = \hbar\omega_{\text{CdSe}} = 60 \text{ cm}^{-1}$ (see table 1). While calculating the transition band at 300 K, $N_1 = 4600$ and $N_2 = 2800$ vibronic levels which originate from the states 5E and 5T_2 and fall into the ranges $\Delta E({}^5E) = 4000 \text{ cm}^{-1}$ and $\Delta E({}^5T_2) = 812 \text{ cm}^{-1}$, respectively, were taken into account. So the full number N_{tot} of examined vibronic transitions that form the ${}^5T_2 \rightarrow {}^5E$ absorption band at 300 K was $N_2 = 12\,880\,000$. In the following in the sums over the Bessel functions n was taken in the limits $-30 \leq n \leq 30$. Figure 3 represents the absorption spectra $K_1(\Omega) \sim \Omega F_1(\Omega)$ ($K_1(\Omega)$ is the absorption coefficient) of the CrSe₄ species at 300 K. A reasonably fair agreement with the experimental data [5] was obtained for $Dq = -395 \text{ cm}^{-1}$ and vibronic coupling constants $v_{T_2}^{(1)}(T_2) = 300 \text{ cm}^{-1}$, $v_E(\text{E}) = 100 \text{ cm}^{-1}$ and $v_{A_1}(\text{E}) = -100 \text{ cm}^{-1}$. The values of the vibronic parameters obtained by fitting are close

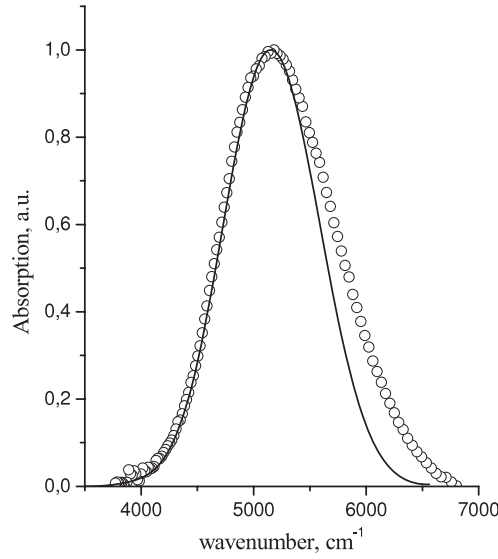


Figure 3. Absorption spectrum of the CdSe:Cr²⁺ crystal at $T = 300$ K: circles, experimental data [5]; solid line, calculated spectra in the case of $\nu_E(E) = 100$ cm⁻¹, $\nu_{T_2}^{(1)}(T_2) = 300$ cm⁻¹, $\nu_{A_1}(E) = -100$ cm⁻¹, $Dq = -395$ cm⁻¹.

to those calculated in the exchange charge model (see table 2). The obtained result serves as a convincing confirmation that the model employed describes reasonably the contribution of the CrSe₄ species to the observed absorption spectra of CdSe_{0.6}S_{0.4}:Cr²⁺.

5. Contribution from the CrSe₃S and CrSeS₃ impurity clusters to the absorption band

5.1. CrSe₃S complex

When one of the four Se atoms is replaced by a S atom the symmetry of the ligand surroundings, as was stated above, is lowered to C_{3v} from T_d. The crystal field operator written in the frame of reference related to the C₃ axis (figure 1(c)) looks as follows:

$$\begin{aligned}
 V_{CF}(C_{3v}) = \frac{2e^2\sqrt{\pi}}{405(R_0R)^5} \left\{ -81\sqrt{5}R^2(A_2^- + 2B_2^-)Y_{20}(\theta, \varphi) \right. \\
 + \frac{2\sqrt{70}}{R_0^4} [5(A_4^+ + A_4^-) + 18(B_4^+ + B_4^-)][Y_{43}(\theta, \varphi) - Y_{4-3}(\theta, \varphi)] \\
 \left. + [14(5A_4^+ + 18B_4^+) - 13(5A_4^- + 18B_4^-)]Y_{40}(\theta, \varphi) \right\}, \quad (27)
 \end{aligned}$$

where

$$A_p^\pm = \langle r^p \rangle Z(R_0^{p+1} \pm R^{p+1}), \quad B_p^\pm = (R_0R)^p G[R_0S_p(R) \pm RS_p(R_0)].$$

In the trigonal crystal field (27) the ground ⁵T₂ term of Cr²⁺ splits into two levels, ⁵E⁽¹⁾ and ⁵A₁, while the excited state ⁵E state remains unsplit (figure 2(c)). The wavefunctions of

Table 3. Vibronic coupling constants (in cm^{-1}) for the CrSe_3S complex.

$v_{A_1}^{(1)}(^5A_1)$			$v_{A_1}^{(2)}(^5A_1)$			$v_{A_1}^{(1)}(^5E)$			$v_{A_1}^{(2)}(^5E)$		
pc	ec	Total	pc	ec	Total	pc	ec	Total	pc	ec	Total
24	50	74	83	148	231	-16	-49	-65	-2	-6	-8
$v_{A_1}^{(1)}(^5E)$			$v_{A_1}^{(2)}(^5E)$			$v_{E(1)}(^5E)$			$v_{E(2)}(^5E)$		
pc	ec	Total	pc	ec	Total	pc	ec	Total	pc	ec	Total
-40	-99	-139	-85	-154	-239	55	11	66	-0.3	0.1	-0.2

these levels have the form

$$\begin{aligned}
|{}^5E_x\rangle &= \frac{1}{\sqrt{2}}(-|x_1x_0x_{-1}u_1\rangle + |x_1x_0x_{-1}u_{-1}\rangle), \\
|{}^5E_x^{(1)}\rangle &= \frac{1}{\sqrt{2}}(-|x_1x_0u_{-1}u_1\rangle + |x_0x_{-1}u_{-1}u_1\rangle), \\
|{}^5A_1\rangle &= |x_1x_{-1}u_{-1}u_1\rangle.
\end{aligned} \tag{28}$$

In equation (28) for each degenerate term the only wavefunction is given; the basis is related to the C_3 axis of the distorted tetrahedron. The trigonal one-electron states (complex trigonal basis) relevant to this coordinate system are expressed in terms of the d-functions $\xi = yz$, $\eta = xz$, $\zeta = xy(t_{2g})$, $u = 3z^2 - r^2$, $v = \sqrt{3}(x^2 - y^2)(e_g)$ defined in the tetragonal basis as follows:

$$\begin{aligned}
|x_+\rangle &= -(1/\sqrt{3})(\varepsilon\xi + \varepsilon^*\eta + \zeta), & |x_-\rangle &= (1/\sqrt{3})(\varepsilon^*\xi + \varepsilon\eta + \zeta), \\
|x_0\rangle &= (1/\sqrt{3})(\xi + \eta + \zeta), & u_+ &= -(1/\sqrt{2})(u + iv), \\
u_- &= (1/\sqrt{2})(u - iv), & \varepsilon &= \exp(2\pi i/3).
\end{aligned} \tag{29}$$

The energy gaps $E(^5E^{(1)}) - E(^5A_1) = 915 \text{ cm}^{-1}$ and $E(^5E) - E(^5A_1) = 4726 \text{ cm}^{-1}$ were calculated using the crystal field potential (27), the wavefunctions (28), (29) and the parameters given in table 1. The obtained $E(^5E^{(1)}) - E(^5A_1)$ gap value appreciably exceeds the thermal energy at room temperature and, thus, the absorption band originating from CrSe_3S species can be assigned to the optical transition ${}^5A_1 \rightarrow {}^5E$. The 5A_1 term interacts with the $A_1^{(1)}$ and $A_1^{(2)}$ vibrations of the surrounding ligands, while the 5E term in addition to these two modes interacts with the $E^{(1)}$ and $E^{(2)}$ modes. At the next step we employ the standard procedure [12, 13] of shifting the reference points of the symmetrized coordinates $q_{A_1}^{(1)}$ and $q_{A_1}^{(2)}$ in (3) to the nuclear configurations consistent with the ground 5A_1 state and introduce new vibrational coordinates $Q_{A_1^{(i)}} = q_{A_1}^{(i)} + v_{A_1}^{(i)}(^5A_1)/\hbar\omega$, $Q_{A_1^{(2)}} = q_{A_1}^{(2)} + v_{A_1}^{(2)}(^5A_1)/\hbar\omega$ ($v_{A_1}^{(i)}(^5A_1) = \langle {}^5A_1 | v_{A_1^{(i)}}(\mathbf{r}) | {}^5A_1 \rangle$, ($i = 1, 2$)) and vibrational operators $v_{A_1^{(i)}}(\mathbf{r}) = v_{A_1^{(i)}}(\mathbf{r}) - v_{A_1^{(i)}}(^5A_1)$, $v_{A_1^{(2)}}(\mathbf{r}) = v_{A_1^{(2)}}(\mathbf{r}) - v_{A_1^{(2)}}(^5A_1)$ corresponding to these modes. Such a procedure is identical to that described in section 4 for the CrSe_4 species (see equations (11)–(13)) and, therefore, we omit its description here. The redefinition of the operators corresponding to $A_1^{(1)}$ and $A_1^{(2)}$ leads to $v_{A_1}^{(i)}(^5A_1) = \langle {}^5A_1 | v_{A_1^{(i)}}(\mathbf{r}) | {}^5A_1 \rangle = 0$ and $v_{A_1}^{(i)}(^5E) = v_{A_1}^{(i)}(^5E) - v_{A_1^{(i)}}(^5A_1)$, where $v_{A_1}^{(i)}(^5E) = \langle {}^5E \parallel v_{A_1^{(i)}}(\mathbf{r}) \parallel {}^5E \rangle / \sqrt{2}$, ($i = 1, 2$). The evaluation of the corresponding vibronic coupling constants was performed in the exchange charge model of the crystal field [12–16]. In table 3 for each vibronic constant the contributions arising from the exchange and point charge fields are indicated. From table 3 it is seen that the interaction of the 5E state with the $E^{(2)}$ vibration is weak in comparison with those with $A_1^{(1)}$, $A_1^{(2)}$ and $E^{(1)}$ vibrations. Therefore, this interaction will not be taken into account in further calculations.

The electron-vibrational wavefunction corresponding to the 5A_1 state can be represented as

$$\Psi({}^5A_1, n_{A_1}^{(1)} n_{A_1}^{(2)} n_{E_x} n_{E_y}) = |{}^5A_1\rangle \Phi_{n_{A_1}^{(1)}}(Q_{A_1}^{(1)}) \Phi_{n_{A_1}^{(2)}}(Q_{A_1}^{(2)}) \Phi_{n_{E_x}}(q_{E_x}) \Phi_{n_{E_y}}(q_{E_y}), \quad (30)$$

where $\Phi_{n_{A_1}^{(i)}}(Q_{A_1}^{(i)})$, etc, are the wavefunctions of the harmonic oscillator. The corresponding energies appear as follows

$$E^{A_1}(n_{A_1}^{(1)}, n_{A_1}^{(2)}, n_{E_x}, n_{E_y}) = -\frac{(v_{A_1}^{(1)}({}^5A_1))^2}{2\hbar\omega} - \frac{(v_{A_1}^{(2)}({}^5A_1))^2}{2\hbar\omega} + \hbar\omega\left(n_{A_1}^{(1)} + \frac{1}{2}\right) + \hbar\omega\left(n_{A_1}^{(2)} + \frac{1}{2}\right) + \hbar\omega\left(n_{E_x} + \frac{1}{2}\right) + \hbar\omega\left(n_{E_y} + \frac{1}{2}\right). \quad (31)$$

The vibronic Hamiltonian for the $E \otimes (e + a_1^{(1)} + a_1^{(2)})$ problem in the 5E state takes on the form

$$H_{ev}({}^5E) = v_E^{(1)}({}^5E)(O_{E_x} q_{E_x} + O_{E_y} q_{E_y}) + v_{A_1}^{(1)}({}^5E)O_{A_1} Q_{A_1}^{(1)} + v_{A_1}^{(2)}({}^5E)O_{A_1} Q_{A_1}^{(2)}, \quad (32)$$

where the elements of the matrices $O_{\Gamma\bar{\gamma}}$ represent the Clebsch–Gordan coefficients $\langle \Gamma\gamma | O_{\Gamma\bar{\gamma}} | \Gamma'\gamma' \rangle = \langle \Gamma\gamma | \Gamma'\gamma' \bar{\Gamma}\bar{\gamma} \rangle$ for the C_{3v} point symmetry group [20]

$$O_{E_x} = \frac{1}{\sqrt{2}} \begin{pmatrix} 0 & 1 \\ 1 & 0 \end{pmatrix}, \quad O_{E_y} = \frac{1}{\sqrt{2}} \begin{pmatrix} 1 & 0 \\ 0 & -1 \end{pmatrix},$$

$v_E^{(1)}({}^5E) = \langle {}^5E \parallel v_E^{(1)}(\mathbf{r}) \parallel {}^5E \rangle / \sqrt{2}$. The hybrid vibronic functions corresponding to the dynamical JT problem in the excited 5E term are written as

$$\Psi_v^E(n_{A_1}^{(1)}, n_{A_1}^{(2)}) = \Phi_{n_{A_1}^{(1)}}(Q_{A_1}^{(1)} - Q_{A_1}^{(1)0}) \Phi_{n_{A_1}^{(2)}}(Q_{A_1}^{(2)} - Q_{A_1}^{(2)0}) \sum_{\substack{\gamma=x,y \\ n_{E_x}, n_{E_y}}} C_v^E(\gamma, n_{E_x}, n_{E_y}) \times \Phi_{n_{E_x}}(q_{E_x}) \Phi_{n_{E_y}}(q_{E_y}) |\gamma\rangle. \quad (33)$$

Here $Q_{A_1}^{(1)0} = -\frac{v_{A_1}^{(1)}({}^5E)}{\hbar\omega} \equiv a_1^{(5E)}$, $Q_{A_1}^{(2)0} = -\frac{v_{A_1}^{(2)}({}^5E)}{\hbar\omega} \equiv a_2^{(5E)}$. The energies of the vibronic states $\Psi_v^E(n_{A_{11}}, n_{A_{12}})$ are

$$\varepsilon(n_{A_1}^{(1)}, n_{A_1}^{(2)}, \nu) = \Delta_1^{(5E)} + \hbar\omega\left(n_{A_1}^{(1)} + \frac{1}{2}\right) + \hbar\omega\left(n_{A_1}^{(2)} + \frac{1}{2}\right) + \varepsilon_\nu^E, \quad (34)$$

where $\Delta_1^{(5E)} = \Delta - ((v_{A_1}^{(1)}({}^5E))^2 + (v_{A_1}^{(2)}({}^5E))^2) / (2\hbar\omega)$, Δ is the crystal field energy gap between the states 5E and 5A_1 and ε_ν^E are the eigenvalues of the ${}^5E \otimes e$ JT vibronic problem. For the numerical solution of this problem the vibronic matrix was truncated, the number N of the harmonic oscillator states satisfied the condition $n_x + n_y \leq N$, where in calculations N was taken to be equal to 60. The general dimension of the matrix was 3782×3782 . The Lanczos method was applied for calculation of the hybrid vibronic states and wavefunctions. The procedure of derivation of the formula for the absorption band shape is described in detail in section 4. Therefore, we do not go into details below. Performing the transformations similar to those in section 4 we obtain the following expression for the shape of the absorption band arising from the $\text{CdSe}_3\text{S:Cr}^{2+}$ species:

$$F_2(\Omega) = \frac{1}{Z_2} \text{Exp} \left[-\frac{(a_1^{(5E)})^2}{2} \coth\left(\frac{\beta}{2}\right) \right] \text{Exp} \left[-\frac{(a_2^{(5E)})^2}{2} \coth\left(\frac{\beta}{2}\right) \right] \times \sum_{\substack{\nu, n_{A_{11}}, n_{A_{12}}, \\ n_{E_x}, n_{E_y}}} \text{Exp} \left[-\frac{E^{A_1}(n_{A_{11}}, n_{A_{12}}, n_{E_x}, n_{E_y})}{kT} \right] \left\{ \frac{1}{3} |C_v^E(E_u, n_{E_x}, n_{E_y})|^2 \right.$$

$$\begin{aligned}
& + \frac{1}{3} |C_v^E(E_v, n_{E_x}, n_{E_y})|^2 \left\{ \sum_{n_1=-\infty}^{\infty} \sum_{n_2=-\infty}^{\infty} I_{n_1} \left(\frac{(a_1^{(5E)})^2}{2Sh(\beta/2)} \right) I_{n_2} \left(\frac{(a_2^{(5E)})^2}{2Sh(\beta/2)} \right) \right. \\
& \times \text{Exp} \left[\frac{n_1 \beta}{2} \right] \text{Exp} \left[\frac{n_2 \beta}{2} \right] \frac{1}{\sqrt{2\pi\lambda^2}} \\
& \times \text{Exp} \left[-\frac{(\Delta_1 + \hbar\omega(n_1 + n_2) - \hbar\omega(n_{E_x} + n_{E_y} + 1) + \varepsilon_v^E - \hbar\Omega)^2}{2\lambda^2} \right] \\
& \times \frac{|\langle {}^5E \parallel d_E \parallel {}^5A_1 \rangle|^2}{2}, \tag{35}
\end{aligned}$$

where $\langle {}^5E \parallel d_E \parallel {}^5A_1 \rangle$ is the matrix element of the effective dipole moment, the symbol d_E denotes the component of the dipole moment which transforms according to the irreducible representation E of the C_{3v} point group; as in (22) the averaging over the light polarization was performed while deriving (35). Finally,

$$Z_2 = \text{Exp} \left(\frac{(v_{A_1}^{(1)}({}^5A_1))^2 + (v_{A_1}^{(2)}({}^5A_1))^2}{2\hbar\omega kT} \right) \frac{1}{4 \sinh^2(\beta/2)} \tag{36}$$

is the partition function for the ground states (31). In calculations for species $\text{CrSe}_{4-y}\text{S}_y$ ($y = 0-3$) the vibrational frequency was approximately taken as

$$\hbar\omega = \hbar\omega_{\text{CdSe}} \sqrt{\frac{m_{\text{Se}}(4m_{\text{Cd}} + (m_{\text{Se}}(4-y) + m_{\text{S}}y))}{(m_{\text{Se}} + m_{\text{Cd}})(m_{\text{Se}}(4-y) + m_{\text{S}}y)}}.$$

In the limiting cases of $y = 0$ and 4 this expression gives a reasonable result: $\hbar\omega = \hbar\omega_{\text{CdSe}} = 60 \text{ cm}^{-1}$

$$\hbar\omega_{\text{CdS}} = \hbar\omega_{\text{CdSe}} \sqrt{\frac{m_{\text{Se}}(m_{\text{Cd}} + m_{\text{S}})}{m_{\text{S}}(m_{\text{Cd}} + m_{\text{Se}})}} \approx 80 \text{ cm}^{-1}.$$

The latter coincides with the value known from literature [6] and given in table 1.

In figure 4 the calculated spectra arising from different species $\text{CrSe}_{4-y}\text{S}_y$ ($y = 1-3$) with mixed ligand surroundings are shown. The contribution $K_2(\Omega) \sim \Omega F_2(\Omega)$ of the CrSe_3S species to the absorption spectra ($K_2(\Omega)$ is the absorption coefficient) of the $\text{CdSe}_{0.6}\text{S}_{0.4}:\text{Cr}^{2+}$ crystal has been calculated with the aid of parameters given in tables 1 and 3. It is seen that this contribution is significant (figure 4). The maximum of the band arising from this species is blue shifted as compared with that belonging to the band from CrSe_4 species.

5.2. CrSeS_3 complex

The symmetry of the impurity complex CrSeS_3 is also C_{3v} . The trigonal crystal field splits the state 5T_2 into two levels ${}^5E^{(1)}$ and 5A_1 , with ${}^5E^{(1)}$ being the ground state (figure 2(d)). The splitting of the 5T_2 state can be described by the crystal field operator (27) if a substitution $R \rightleftharpoons R_0$ is made. However, now the order of the levels ${}^5E^{(1)}$ and 5A_1 is reversed as compared to the case of the CrSe_3S species (figure 2(c)). The calculated energy gap 932 cm^{-1} between the states ${}^5E^{(1)}$ and 5A_1 is large in comparison with the thermal energy and the absorption band is formed by the only transition ${}^5E^{(1)} \rightarrow {}^5E$. To determine the vibronic problems to be solved for these levels the vibronic coupling constants have been calculated (table 4) with the aid of wavefunctions (28) and corresponding vibrational operators. The redefinition of the vibronic operators $A_1^{(1)}$ and $A_1^{(2)}$ similar to that described in section 5.1 (see also (12)

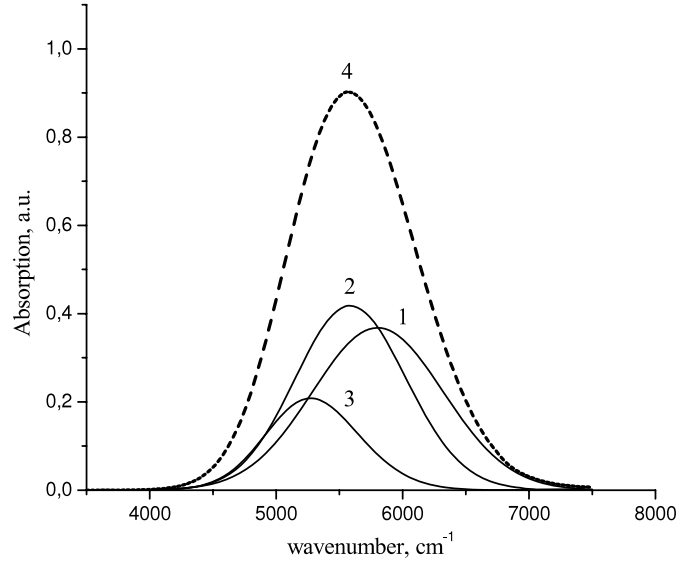


Figure 4. Calculated contributions from species with mixed ligand surroundings of the Cr^{2+} ion to the total absorption spectra at $T = 300$ K: 1, CrSe_3S_1 ; 2, CrSe_2S_2 ; 3, CrSe_1S_3 ; 4, total spectrum arising from $\text{CrSe}_{4-y}\text{S}_y$ species ($y = 1-3$).

Table 4. Vibronic coupling constants (in cm^{-1}) for the CrSeS_3 complex.

$\nu_{A_1}^{(1)}(^5E^{(1)})$			$\nu_{A_1}^{(2)}(^5E^{(1)})$			$\nu_E^{(1)}(^5E^{(1)})$			$\nu_E^{(2)}(^5E^{(1)})$		
pc	ec	Total	pc	ec	Total	pc	ec	Total	pc	ec	Total
14	45	59	-40	-74	-114	-9	-72	-81	19	37	56
$\nu_{A_1}^{(1)}(^5E)$			$\nu_{A_1}^{(2)}(^5E)$			$\nu_{A_1}^{(1)}(^5E)$			$\nu_{A_1}^{(2)}(^5E)$		
pc	ec	Total	pc	ec	Total	pc	ec	Total	pc	ec	Total
-20	-59	-79	1	5	6	-34	-104	-138	41	79	120
$\nu_E^{(1)}(^5E)$			$\nu_E^{(2)}(^5E)$								
pc	ec	Total	pc	ec	Total						
61	12	73	10	2	12						

and (13)) leads to vanishing vibronic constants $\nu_{A_1}^{(i)}(^5E^{(1)})$ ($i = 1, 2$) for the ground $^5E^{(1)}$ state and $\nu_{A_1}^{(1)}(^5E) = -138 \text{ cm}^{-1}$, $\nu_{A_1}^{(2)}(^5E) = 120 \text{ cm}^{-1}$ for the excited 5E state. For both $^5E^{(1)}$ and 5E terms the interaction with the $E^{(1)}$ mode is stronger than that with the $E^{(2)}$ mode. Therefore, in further calculations we consider only the interaction of these terms with the $E^{(1)}$ mode. For the ground $^5E^{(1)}$ term the Hamiltonian of vibronic interaction looks as follows

$$H_{ev}(^5E^{(1)}) = \nu_E^{(1)}(^5E^{(1)})(q_{E_x}\mathbf{O}_{E_x} + q_{E_y}\mathbf{O}_{E_y}). \quad (37)$$

In fact we solve the vibronic two-mode $E \otimes e$ problem with the interaction constant $\nu_E^{(1)}(^5E^{(1)}) = -100 \text{ cm}^{-1}$ which slightly differs from the calculated one (see table 4). The eigenvalues and eigenvectors for this problem can be written as

$$\begin{aligned}
E_v^{gr}(n_{A_1^{(1)}}, n_{A_1^{(2)}}) &= -\frac{(v_{A_1^{(1)}}^{(1)}(\delta E^{(1)}))^2}{2\hbar\omega} - \frac{(v_{A_1^{(2)}}^{(2)}(\delta E^{(1)}))^2}{2\hbar\omega} + \hbar\omega\left(n_{A_1^{(1)}} + \frac{1}{2}\right) \\
&\quad + \hbar\omega\left(n_{A_1^{(2)}} + \frac{1}{2}\right) + \varepsilon_v^{gr}, \\
\Psi_v^{gr}(n_{A_1^{(1)}}, n_{A_1^{(2)}}) &= \Phi_{n_{A_1^{(1)}}}^{(1)}(Q_{A_1^{(1)}})\Phi_{n_{A_1^{(2)}}}^{(2)}(Q_{A_1^{(2)}}) \sum_{\substack{\gamma=x,y \\ n_{E_x}, n_{E_y}}} C_v^{gr}(\gamma, n_{E_x}, n_{E_y}) \\
&\quad \times \Phi_{n_{E_x}}(q_{E_x})\Phi_{n_{E_y}}(q_{E_y})|\gamma\rangle,
\end{aligned} \tag{38}$$

where the values ε_v^{gr} will be determined from the solution of the $E \otimes e$ JT problem for the ${}^5E^{(1)}$ term, $v_{A_1^{(i)}}^{(i)}(\delta E^{(1)}) = \langle \delta E^{(1)} \parallel v_{A_1^{(i)}}^{(i)}(\mathbf{r}) \parallel {}^5E^{(1)} \rangle / \sqrt{2}$, ($i = 1, 2$). For the 5E term the vibronic $E \otimes (e + a_1^{(1)} + a_1^{(2)})$ problem is examined, the eigenvectors and eigenfunctions complying with this problem can be represented as

$$\begin{aligned}
E_v^{ex}(n_{A_1^{(1)}}, n_{A_1^{(2)}}) &= \Delta - \frac{(v_{A_1^{(1)}}^{(1)}(\delta E))^2}{2\hbar\omega} - \frac{(v_{A_1^{(2)}}^{(2)}(\delta E))^2}{2\hbar\omega} + \hbar\omega\left(n_{A_1^{(1)}} + \frac{1}{2}\right) \\
&\quad + \hbar\omega\left(n_{A_1^{(2)}} + \frac{1}{2}\right) + \varepsilon_v^{ex}, \\
\Psi_v^{ex}(n_{A_1^{(1)}}, n_{A_1^{(2)}}) &= \Phi_{n_{A_1^{(1)}}}^{(1)}(Q_{A_1^{(1)}} - \tilde{Q}_{A_1^{(1)}}^0)\Phi_{n_{A_1^{(2)}}}^{(2)}(Q_{A_1^{(2)}} - \tilde{Q}_{A_1^{(2)}}^0) \\
&\quad \times \sum_{\substack{\gamma=x,y \\ n_{E_x}, n_{E_y}}} C_v^{ex}(\gamma, n_{E_x}, n_{E_y})\Phi_{n_{E_x}}(q_{E_x})\Phi_{n_{E_y}}(q_{E_y})|\gamma\rangle,
\end{aligned} \tag{39}$$

where

$$\begin{aligned}
\tilde{Q}_{A_1^{(1)}}^0 &= -\tilde{v}_{A_1^{(1)}}^{(1)}(\delta E)/(\hbar\omega) \equiv \tilde{a}_1^{(\delta E)}, & \tilde{Q}_{A_1^{(2)}}^0 &= -\tilde{v}_{A_1^{(2)}}^{(2)}(\delta E)/(\hbar\omega) \equiv \tilde{a}_2^{(\delta E)}, \\
\tilde{v}_{A_1^{(i)}}^{(i)}(\delta E) &= v_{A_1^{(i)}}^{(i)}(\delta E) - v_{A_1^{(i)}}^{(i)}(\delta E^{(1)}),
\end{aligned}$$

and ε_v^{ex} is the solution of the $E \otimes e$ problem for the 5E term. While solving the vibronic $E \otimes e$ problems for the initial and final terms of the optical transition ${}^5E^{(1)} \rightarrow {}^5E$ the condition $n_{E_x} + n_{E_y} \leq N$ ($N = 60$) was retained as in the case of CrSe_3S species. The shape $F_3(\Omega)$ of the absorption band arising from the impurity cluster CrSe_3S is given by the expression

$$\begin{aligned}
F_3(\Omega) &= \frac{1}{Z_4} \text{Exp} \left[-\frac{(\tilde{a}_1^{(\delta E)})^2}{2} \coth\left(\frac{\beta}{2}\right) \right] \text{Exp} \left[-\frac{(\tilde{a}_2^{(\delta E)})^2}{2} \coth\left(\frac{\beta}{2}\right) \right] \sum_{v,v'} \text{Exp} \left[-\frac{E_v^{E_{gr}}}{kT} \right] \\
&\quad \times \left\{ \sum_{n_{E_x}, n_{E_y}} [(C_{v'}^{ex}(x, n_{E_x}, n_{E_y}))^* C_v^{gr}(x, n_{E_x}, n_{E_y}) + (C_{v'}^{ex}(y, n_{E_x}, n_{E_y}))^* \right. \\
&\quad \times C_v^{gr}(y, n_{E_x}, n_{E_y})]^2 \frac{|\langle \delta E \parallel d_E \parallel {}^5E^{(1)} \rangle|^2}{4} + \sum_{n_{E_x}, n_{E_y}} [(C_{v'}^{ex}(x, n_{E_x}, n_{E_y}))^* \\
&\quad \times C_v^{gr}(y, n_{E_x}, n_{E_y}) + (C_{v'}^{ex}(y, n_{E_x}, n_{E_y}))^* C_v^{gr}(x, n_{E_x}, n_{E_y})]^2 \\
&\quad \times \frac{|\langle \delta E \parallel d_E \parallel {}^5E^{(1)} \rangle|^2}{4} + \sum_{n_{E_x}, n_{E_y}} [(C_{v'}^{ex}(x, n_{E_x}, n_{E_y}))^* C_v^{gr}(y, n_{E_x}, n_{E_y}) \\
&\quad \left. - (C_{v'}^{ex}(y, n_{E_x}, n_{E_y}))^* C_v^{gr}(x, n_{E_x}, n_{E_y})]^2 \frac{|\langle \delta E \parallel d_{A_2} \parallel {}^5E^{(1)} \rangle|^2}{2} \right\} \\
&\quad \times \sum_{n_1=-\infty}^{\infty} \sum_{n_2=-\infty}^{\infty} I_{n_1} \left(\frac{(\tilde{a}_1^{(\delta E)})^2}{2Sh(\beta/2)} \right) I_{n_2} \left(\frac{(\tilde{a}_2^{(\delta E)})^2}{2Sh(\beta/2)} \right) \text{Exp} \left[\frac{n_1\beta}{2} \right] \text{Exp} \left[\frac{n_2\beta}{2} \right] \\
&\quad \times \frac{1}{\sqrt{2\pi\lambda^2}} \text{Exp} \left[-\frac{(\tilde{E}_{v'}^{ex} - \tilde{E}_v^{gr} + \hbar\omega(n_1 + n_2) - \hbar\Omega)^2}{2\lambda^2} \right], \tag{40}
\end{aligned}$$

where

$$\begin{aligned}\tilde{E}_v^{gr} &= -\frac{(v_{A_1}^{(1)}(\langle^5E^{(1)}\rangle)^2)}{2\hbar\omega} - \frac{(v_{A_1}^{(2)}(\langle^5E^{(1)}\rangle)^2)}{2\hbar\omega} + \varepsilon_v^{gr}, \\ \tilde{E}_v^{ex} &= \Delta - \frac{(v_{A_1}^{(1)}(\langle^5E\rangle)^2)}{2\hbar\omega} - \frac{(v_{A_1}^{(2)}(\langle^5E\rangle)^2)}{2\hbar\omega} + \varepsilon_v^{ex}, \\ Z_4 &= \sum_v \text{Exp}\left[-\frac{\tilde{E}_v^{gr}}{kT}\right],\end{aligned}$$

where the notation $\langle^5E \parallel d_E \parallel ^5E^{(1)}\rangle$ has the same sense as in (3) and $\langle^5E \parallel d_{A_2} \parallel ^5E^{(1)}\rangle$ is the reduced matrix element of the dipole moment component that transforms according to the irreducible representation A_2 of the C_{3v} point group. The partial contribution $K_3(\Omega) \sim \Omega F_3(\Omega)$ of the CrSe_3S_3 species was calculated with the aid of parameters given in tables 1 and 4 and it is depicted in figure 4 (curve 3). It is obvious that this species also give a blue shifted band relative to that originating from the CrSe_4 one. At the same time the intensity of this band is lower in comparison with the intensity of the band belonging to the CrSe_3S cluster.

6. Absorption band of the impurity CrSe_2S_2 cluster

When the nearest neighbour surrounding of the Cr^{2+} ion consists of two selenium and two sulfur atoms the symmetry of the impurity complex is C_{2v} and the crystal field potential looks as follows

$$\begin{aligned}V_{\text{CF}}(C_{2v}) &= \frac{ie^2\sqrt{\pi}}{135(R_0R)^5} \{i\sqrt{70}(5A_4^+ + 18B_4^+)[Y_{44}(\theta, \varphi) + Y_{4-4}(\theta, \varphi)] \\ &\quad + 4\sqrt{10}(5A_4^- + 18B_4^-)[Y_{42}(\theta, \varphi) - Y_{4-2}(\theta, \varphi)] \\ &\quad + 14i(5A_4^+ + 18B_4^+)Y_{40}(\theta, \varphi) \\ &\quad + 18\sqrt{30}R_0^2R^2(A_2^- + 2B_2^-)[Y_{22}(\theta, \varphi) - Y_{2-2}(\theta, \varphi)]\},\end{aligned}\quad (41)$$

where the functions A_p^\pm and B_p^\pm are determined in (27). In this case the energy spectrum of the Cr^{2+} ion consists of five levels $^5A_1^{(1)}$, 5A_2 , 5B_2 , 5B_1 , $^5A_1^{(2)}$. The states $^5A_1^{(1)}$ and 5A_2 originate from the cubic 5E state, while the states 5B_2 , 5B_1 , $^5A_1^{(2)}$ arise from the splitting of the ground 5T_2 term (figure 2(b)). The wavefunctions of these states are

$$\begin{aligned}|^5A_2\rangle &= -|u\xi\eta\zeta\rangle, &|^5A_1^{(1)}\rangle &= C_1|\xi\eta uv\rangle + C_2|v\xi\eta\zeta\rangle, \\|^5B_1\rangle &= (|\xi\zeta uv\rangle - |\eta\zeta uv\rangle)/\sqrt{2}, &|^5B_2\rangle &= (|\xi\zeta uv\rangle + |\eta\zeta uv\rangle)/\sqrt{2}, \\|^5A_1^{(2)}\rangle &= -C_2|\xi\eta uv\rangle + C_1|v\xi\eta\zeta\rangle,\end{aligned}\quad (42)$$

where the coefficients C_1 and C_2 can be obtained from the diagonalization of the crystal field potential (41). The energies of the levels $^5A_1^{(1)}$, 5A_2 , 5B_2 , 5B_1 , $^5A_1^{(2)}$ in the crystal field have been calculated with the aid of the crystal field potential (41), wavefunctions (42) and overlap integrals given in table 1. The obtained energy gaps between the ground 5B_1 level and the excited $^5A_1^{(2)}$ and 5B_2 ones exceed essentially the thermal energy, and the absorption band of the CrSe_2S_2 cluster at room temperature arises from the optical transitions $^5B_1 \rightarrow ^5A_2$, $^5B_1 \rightarrow ^5A_1^{(1)}$ between orbitally nondegenerate states interacting with one-dimensional vibrations. While calculating the structure of the multiphonon absorption band the interaction of the terms 5B_1 , 5A_2 and $^5A_1^{(1)}$ with the vibrations $A_1^{(1)}$, $A_1^{(2)}$ and $A_1^{(3)}$ was

Table 5. Vibronic coupling constants (in cm^{-1}) for the CrSe_2S_2 complex.

$\nu_{A_1}^{(1)}(^5B_1)$			$\nu_{A_1}^{(2)}(^5B_1)$			$\nu_{A_1}^{(3)}(^5B_1)$		
pc	ec	Total	pc	ec	Total	pc	ec	Total
17	36	53	70	131	201	16	2	18
$\nu_{A_1}^{(1)}(^5A_1^{(1)})$			$\nu_{A_1}^{(2)}(^5A_1^{(1)})$			$\nu_{A_1}^{(3)}(^5A_1^{(1)})$		
pc	ec	Total	pc	ec	Total	pc	ec	Total
-17	-52	-69	2	-15	-13	63	18	81
$\nu_{A_1}^{(1)}(^5A_1^{(1)})$			$\nu_{A_1}^{(2)}(^5A_1^{(1)})$			$\nu_{A_1}^{(3)}(^5A_1^{(1)})$		
pc	ec	Total	pc	ec	Total	pc	ec	Total
-34	-88	-122	-68	-146	-214	47	16	63
$\nu_{A_1}^{(1)}(^5A_2)$			$\nu_{A_1}^{(2)}(^5A_2)$			$\nu_{A_1}^{(3)}(^5A_2)$		
pc	ec	Total	pc	ec	Total	pc	ec	Total
-19	-53	-72	-15	-17	-32	-58	-8	-66
$\nu_{A_1}^{(1)}(^5A_2)$			$\nu_{A_1}^{(2)}(^5A_2)$			$\nu_{A_1}^{(3)}(^5A_2)$		
pc	ec	Total	pc	ec	Total	pc	ec	Total
-36	-89	-125	-85	-148	-233	-74	-10	-84

taken into account. The vibrational coordinates for modes $A_1^{(1)}$, $A_1^{(2)}$, $A_1^{(3)}$ and the vibrational operators corresponding to these modes were redefined:

$$\begin{aligned}
Q_{A_1^{(1)}} &= q_{A_1^{(1)}} + \nu_{A_1^{(1)}}(^5B_1)/\hbar\omega, & Q_{A_1^{(2)}} &= q_{A_1^{(2)}} + \nu_{A_1^{(2)}}(^5B_1)/\hbar\omega, \\
Q_{A_1^{(3)}} &= q_{A_1^{(3)}} + \nu_{A_1^{(3)}}(^5B_1)/\hbar\omega, & \nu_{A_1^{(1)}}(\mathbf{r}) &= \nu_{A_1^{(1)}}(\mathbf{r}) - \nu_{A_1^{(1)}}(^5B_1), \\
\nu_{A_1^{(2)}}(\mathbf{r}) &= \nu_{A_1^{(2)}}(\mathbf{r}) - \nu_{A_1^{(2)}}(^5B_1), & \nu_{A_1^{(3)}}(\mathbf{r}) &= \nu_{A_1^{(3)}}(\mathbf{r}) - \nu_{A_1^{(3)}}(^5B_1),
\end{aligned} \quad (43)$$

here $\nu_{A_1^{(i)}}(^5B_1) = \langle ^5B_1 | \nu_{A_1^{(i)}}(\mathbf{r}) | ^5B_1 \rangle$, ($i = 1-3$). As a result the electron-vibrational energies and states complying with the ground 5B_1 term can be written as

$$\begin{aligned}
E^{5B_1}(n_{A_1^{(1)}}, n_{A_1^{(2)}}, n_{A_1^{(3)}}) &= \varepsilon^{5B_1} + \hbar\omega(n_{A_1^{(1)}} + n_{A_1^{(2)}} + n_{A_1^{(3)}} + \frac{3}{2}), \\
\psi^{5B_1}(n_{A_1^{(1)}}, n_{A_1^{(2)}}, n_{A_1^{(3)}}) &= \Phi_{n_{A_1^{(1)}}}(Q_{A_1^{(1)}})\Phi_{n_{A_1^{(2)}}}(Q_{A_1^{(2)}})\Phi_{n_{A_1^{(3)}}}(Q_{A_1^{(3)}})|^5B_1
\end{aligned} \quad (44)$$

here

$$\varepsilon^{5B_1} = -\frac{1}{2\hbar\omega}((\nu_{A_1^{(1)}}(^5B_1))^2 + (\nu_{A_1^{(2)}}(^5B_1))^2 + (\nu_{A_1^{(3)}}(^5B_1))^2).$$

For the excited states $^5A_1^{(1)}$ and 5A_2 participating in the optical transitions $^5B_1 \rightarrow ^5A_1^{(1)}$, $^5B_1 \rightarrow ^5A_2$ the strongest is the interaction with the $A_1^{(2)}$ mode, at the same time the interaction with the $A_1^{(1)}$ and $A_1^{(3)}$ vibrations is weaker, but appreciable (table 5). For this reason the interaction of the excited terms $^5A_1^{(1)}$ and 5A_2 with all active vibrations is taken into account. The electron-vibrational wavefunctions and corresponding energies for the excited terms $^5A_1^{(1)}$ and 5A_2 are:

$$\begin{aligned}
E^{(\Gamma)}(n_{A_1^{(1)}}, n_{A_1^{(2)}}, n_{A_1^{(3)}}) &= \varepsilon^{(\Gamma)} + \hbar\omega(n_{A_1^{(1)}} + n_{A_1^{(2)}} + n_{A_1^{(3)}} + \frac{3}{2}), \\
\psi^{(\Gamma)}(n_{A_1^{(1)}}, n_{A_1^{(2)}}, n_{A_1^{(3)}}) &= \Phi_{n_{A_1^{(1)}}}(Q_{A_1^{(1)}} - Q_{A_1^{(2)}}^0(\Gamma))\Phi_{n_{A_1^{(2)}}} \\
&\times (Q_{A_1^{(2)}} - Q_{A_1^{(2)}}^0(\Gamma))\Phi_{n_{A_1^{(3)}}}(Q_{A_1^{(3)}} - Q_{A_1^{(3)}}^0(\Gamma))|\Gamma,
\end{aligned} \quad (45)$$

here $\Gamma = {}^5A_1^{(1)}, {}^5A_2$,

$$Q_{A_1^{(i)}}^0(\Gamma) = -\frac{v_{A_1^{(i)}}(\Gamma)}{\hbar\omega} \equiv a_i(\Gamma), \quad v_{A_1^{(i)}}(\Gamma) = v_{A_1^{(i)}}(\Gamma) - v_{A_1^{(i)}}({}^5B_1), \quad (i = 1-3),$$

$$\varepsilon(\Gamma) = \Delta(\Gamma) - \frac{1}{2\hbar\omega} ((v_{A_1^{(1)}}(\Gamma))^2 + (v_{A_1^{(2)}}(\Gamma))^2 + (v_{A_1^{(3)}}(\Gamma))^2).$$

The shape of the absorption band arising from the ${}^5B_1 \rightarrow {}^5A_1^{(1)}$ and ${}^5B_1 \rightarrow {}^5A_2$ transitions is described as follows:

$$\begin{aligned} F_4(\Omega) = & \sum_{\Gamma={}^5A_1^{(1)}, {}^5A_2} \left\{ \frac{1}{3} \text{Exp} \left[-\frac{(a_1(\Gamma))^2}{2} \coth \left(\frac{\beta}{2} \right) \right] \text{Exp} \left[-\frac{(a_2(\Gamma))^2}{2} \coth \left(\frac{\beta}{2} \right) \right] \right. \\ & \times \text{Exp} \left[-\frac{(a_3(\Gamma))^2}{2} \coth \left(\frac{\beta}{2} \right) \right] \sum_{n_1, n_2, n_3=-\infty}^{\infty} I_{n_1} \left(\frac{(a_1(\Gamma))^2}{2Sh(\beta/2)} \right) I_{n_2} \left(\frac{(a_2(\Gamma))^2}{2Sh(\beta/2)} \right) \\ & \times I_{n_3} \left(\frac{(a_3(\Gamma))^2}{2Sh(\beta/2)} \right) \text{Exp} \left[\frac{n_1\beta}{kT} \right] \text{Exp} \left[\frac{n_2\beta}{kT} \right] \text{Exp} \left[\frac{n_3\beta}{kT} \right] \frac{1}{\sqrt{2\pi\lambda^2}} \\ & \left. \times \text{Exp} \left[-\frac{(\varepsilon(\Gamma) - \varepsilon^{5B_1} + \hbar\omega(n_1 + n_2 + n_3) - \hbar\Omega)^2}{2\lambda^2} \right] \frac{|\langle \Gamma \| d_{\tilde{\Gamma}} \| {}^5B_1 \rangle|^2}{2} \right\}, \end{aligned} \quad (46)$$

where $\tilde{\Gamma} = B_1, B_2$ for $\Gamma = {}^5A_1^{(1)}, {}^5A_2$, respectively. The contribution $K_4(\Omega) \sim \Omega F_4(\Omega)$ of the CrSe_2S_2 species to the total absorption spectra was calculated with the aid of parameters given in tables 1 and 5, and it is depicted in figure 4 (curve 2). It is obvious that this species gives the highest contribution to the band arising from impurity chromium clusters with mixed ligand surroundings. The position of the maximum of the band belonging to CrSe_2S_2 species almost coincides with that for the total band (figure 4, curve 4) originating from all $\text{CrSe}_{4-y}\text{S}_y$ ($y = 1-3$) species with mixed ligand surroundings.

7. Comparison of theory and experiment. Concluding remarks

The total absorption spectrum of the $\text{CdSe}_{0.6}\text{S}_{0.4}:\text{Cr}^{2+}$ crystal has been calculated by summation over partial spectra arising from all species described above taking into account their statistical weights obtained in section 2. The form-function of the absorption band arising from the $\text{CdSe}_{0.6}\text{S}_{0.4}:\text{Cr}^{2+}$ system can be presented in the following form:

$$F(\Omega) = P_1 F_1(\Omega) + P_2 F_2(\Omega) + P_3 F_3(\Omega) + P_4 F_4(\Omega), \quad (47)$$

where the numerical values of the probabilities P_i ($i = 1-4$) are given by equation (2). For numerical calculation of the absorption coefficient $K(\Omega) \sim \Omega F(\Omega)$ at 300 K the parameters given in tables 1-5 were used. Insofar as all optical transitions participating in the formation of the absorption band of the $\text{CdSe}_{0.6}\text{S}_{0.4}:\text{Cr}^{2+}$ crystal are symmetry allowed for the first approximation in calculations the values of the matrix elements $|\langle \Gamma \| d_{\tilde{\Gamma}} \| \Gamma' \rangle|^2$ were taken as equal. In figure 5 the experimental and calculated spectra are shown together. Insofar as the theoretical calculations make it possible to separate the contributions of different $\text{CrSe}_{4-y}\text{S}_y$ species ($y = 0-3$) to the total spectrum both the contributions of species with mixed ligand surroundings and CrSe_4 species are presented in figure 5. Figure 5 clearly demonstrates that the main contribution to the absorption spectra comes from species $\text{CrSe}_{4-y}\text{S}_y$ ($y = 1-3$) with mixed ligand surroundings. Namely, these species are responsible for the observed blue shift of the absorption band in the infrared range. Quite good agreement with the experiment was found.

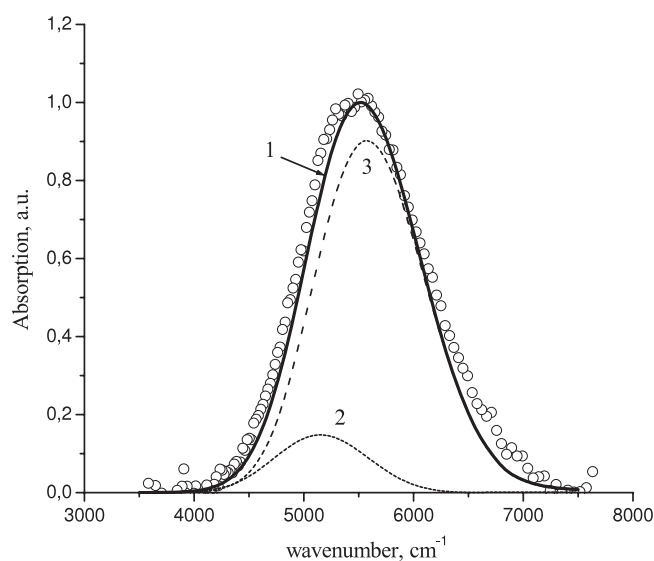


Figure 5. Absorption band of the $\text{CdSe}_{0.6}\text{S}_{0.4}:\text{Cr}^{2+}$ at $T = 300$ K, with circles showing experimental data [5]: 1, total calculated spectrum: 2, partial contribution of the CrSe_4 species: 3, partial contribution of species CrSe_3S_1 , CrSe_2S_2 , CrSe_1S_3 with mixed ligand surroundings.

The results obtained can be summarized as follows. Here we have presented a model of optical spectra of $\text{CdSe}_{0.6}\text{S}_{0.4}:\text{Cr}^{2+}$ crystals that takes into account the possibility of formation of impurity clusters with mixed ligand surroundings. The most probable nearest neighbour arrangements of the Cr^{2+} ion are found to include (i) four selenium atoms, (ii) three selenium and one sulfur atom or three sulfur and one selenium atom, (iii) two selenium and two sulfur atoms. For these arrangements of the Cr^{2+} ion the crystal field acting on this ion and the interaction of the d-electrons with the vibrations of the nearest ligand surroundings were considered in a realistic model of the crystal field with allowance for covalency effects. For all impurity clusters $\text{CrSe}_{4-y}\text{S}_y$ ($y = 0-3$) the crystal field splittings and the vibronic coupling parameters have been microscopically calculated. Then, on this basis the vibronic JT problems have been defined and solved numerically. The total spectrum of the $\text{CdSe}_{0.6}\text{S}_{0.4}:\text{Cr}^{2+}$ crystal calculated by summation over partial spectra arising from all mentioned species is in good agreement with the experimental one.

In order to discuss the real $\text{CdSe}_{0.6}\text{S}_{0.4}:\text{Cr}^{2+}$ system in more detail the adopted model needs to be generalized in several aspects. A new computational approach to the problem of optical spectra of the CrSe_4 cluster that takes into account all active vibrations interacting with Cr^{2+} ion should be developed. In calculations for the clusters $\text{CrSe}_{4-y}\text{S}_y$ ($y = 0-3$), the frequencies of the vibrations were taken in accordance with the composition of the nearest surrounding ligand. This question is also in need of special consideration. In spite of these restricting assumptions, the developed model gives a simultaneous explanation in its framework of the experimental data on both $\text{CdSe}_{0.6}\text{S}_{0.4}:\text{Cr}^{2+}$ and $\text{CdSe}:\text{Cr}^{2+}$ crystals and reflects the main features of the observed spectra.

Acknowledgments

The research described in this publication was made possible in part by Award BGP-III no. MOP2-3056-CS-03 of the Moldovan Research and Development Association (MRDA)

under funding from the US Civilian Research and Development Foundation (CRDF). Financial support of the Supreme Council for Science and Technological Development of Moldova is highly appreciated. The authors thank also Professor B S Tsukerblat for useful discussions about the paper.

Appendix

(a) Symmetry adapted vibrational coordinates for the CdSe₃S:Cr²⁺ complex of C_{3v} symmetry:

$$\begin{aligned}
 q_{A_1}^{(1)} &= \frac{[(2x_1 - x_2 - x_3 + \sqrt{3}y_2 - \sqrt{3}y_3)\sqrt{\frac{m}{12}} - (z_1 + z_2 + z_3)\frac{M}{3\sqrt{m}} + z_4\sqrt{M}]}{\sqrt{M + m + \frac{M^2}{3m}}} \\
 q_{A_1}^{(2)} &= \frac{[-(2x_1 - x_2 - x_3 + \sqrt{3}y_2 - \sqrt{3}y_3)\frac{M}{\sqrt{12m}}(1 + \frac{M}{3m}) - (z_1 + z_2 + z_3)\frac{M}{3\sqrt{m}} + z_4\sqrt{M}]}{\sqrt{\frac{M^2}{m}(1 + \frac{M}{3m}) + \frac{M^2}{3m} + M}} \\
 q_{E_x}^{(1)} &= \frac{[-\frac{M}{3\sqrt{m}}(2x_1 + \frac{x_2}{2} + \frac{x_3}{2} - \frac{\sqrt{3}}{2}y_2 + \frac{\sqrt{3}}{2}y_3) + \sqrt{M}x_4 + \sqrt{\frac{m}{6}}(2z_1 - z_2 - z_3)]}{\sqrt{\frac{2M^2}{3m} + M + m}} \\
 q_{E_x}^{(2)} &= \frac{\frac{M}{3\sqrt{m}}(2x_1 + \frac{x_2}{2} - \frac{\sqrt{3}}{2}y_2 + x_3 + \frac{\sqrt{3}}{2}y_3) + \frac{M}{\sqrt{6m}}(1 + \frac{2M}{3m})(2z_1 - z_2 - z_3) - \sqrt{M}x_4}{\sqrt{\frac{2M^2}{3m} + \frac{M^2}{m}(1 + \frac{2M}{3m})^2 + M}} \\
 q_{E_y}^{(1)} &= \frac{[-\frac{M}{2\sqrt{3m}}(-x_2 + \sqrt{3}y_2 + x_3 + \sqrt{3}y_3) + \sqrt{\frac{m}{2}}(z_2 - z_3) + \sqrt{M}y_4]}{\sqrt{\frac{2M^2}{3m} + M + m}} \\
 q_{E_y}^{(2)} &= \frac{[\frac{M}{2\sqrt{3m}}(-x_2 + y_2 + x_3 + \sqrt{3}y_3) + \frac{M}{\sqrt{2m}}(1 + \frac{2M}{3m})(z_2 - z_3) - \sqrt{M}y_4]}{\sqrt{\frac{2M^2}{3m} + \frac{M^2}{m}(1 + \frac{2M}{3m})^2 + M}}
 \end{aligned} \tag{A.1}$$

where m and M are the masses of selenium and sulfur atoms, respectively. The numbering of ligands in (A.1) and further on corresponds to that given in figure 1.

(b) Symmetry adapted vibrational coordinates for the CdSe₂S₂:Cr²⁺ complex of C_{2v} symmetry

$$\begin{aligned}
 q_{A_1}^{(1)} &= \frac{[(x_1 - x_4 + y_1 - y_4)\sqrt{\frac{M}{4}} + (x_3 - x_2 + y_2 - y_3)\sqrt{\frac{m}{4}} + (z_1 + z_4)\sqrt{\frac{M}{2}} - (z_2 + z_3)\sqrt{\frac{m}{2}}]}{\sqrt{\frac{M^2}{m} + 2M + m}} \\
 q_{A_1}^{(2)} &= \frac{[(x_1 - x_4 + y_1 - y_4)\sqrt{\frac{M}{4}} - (x_3 - x_2 + y_2 - y_3)\frac{M}{\sqrt{4m}}]}{\sqrt{M + \frac{M^2}{m}}} \\
 q_{A_1}^{(3)} &= \frac{[(x_1 - x_4 + y_1 - y_4)\sqrt{\frac{M}{4}} + (x_3 - x_2 + y_2 - y_3)\sqrt{\frac{m}{4}} - \frac{m}{\sqrt{2M}}(z_1 + z_4) + (z_2 + z_3)\sqrt{\frac{m}{2}}]}{\sqrt{M + 2m + \frac{m^2}{M}}} \\
 q_{A_2} &= \frac{[(x_1 - y_1 - x_4 + y_4)\sqrt{\frac{M}{4}} + (x_3 + y_3 - x_2 - y_2)\sqrt{\frac{m}{4}}]}{\sqrt{M + m}}
 \end{aligned}$$

$$q_{B_1} = \frac{[(x_1 + y_1 + x_4 + y_4)\sqrt{\frac{M}{4}} - (x_2 + y_2 + x_3 + y_3)\frac{M}{\sqrt{4m}} + (z_1 - z_4)\sqrt{\frac{M}{4}}]}{\sqrt{\frac{M^2}{m} + 2M}}$$

$$q_{B_2} = \frac{[(x_1 - y_1 + x_4 - y_4)\sqrt{\frac{M}{4}} - (x_2 - y_2 + x_3 - y_3)\frac{M}{\sqrt{4m}}]}{\sqrt{\frac{M^2}{m} + M}}$$

(A.2)

where, as in (A.1), m and M are the masses of the selenium and sulfur atoms, respectively.

The operators $v_{\bar{\mu}\bar{\Gamma}\bar{\gamma}}(\mathbf{r})$ corresponding to the vibrational coordinates $q_{\bar{\mu}\bar{\Gamma}\bar{\gamma}}$ have been obtained with the aid of relations (7) and (A.1), (A.2).

References

- [1] Deloach L D, Page R H, Wilke G D, Payne S A and Krupke W F 1996 *IEEE J. Quantum Electron.* **32** 885
- [2] Page R H, Schaffers K I, Deloach L D, Wilke G D, Patel F D, Tassano J B, Payne S A, Krupke W F, Chen K T and Burger A 1997 *IEEE J. Quantum Electron.* **33/34** 609
- [3] McKay J, Schepler K and Kuck S 1998 *OSA Annual Meeting (Baltimore)* paper ThGG1
Wagner J, Carrig T J, Page R H, Schaffers K I, Ndad J-O, Ma X and Burger A 1999 *Opt. Lett.* **24** 19
Hömmerich U, Wu X, Davis V R, Trivedi S B, Grasza K, Chen R J and Kutcher S 1997 *Opt. Lett.* **22** 1180
Seo J T, Hömmerich U, Zong H, Trivedi S B, Kutcher S W, Wang C C and Chen R J 1999 *Phys. Status Solidi a* **A175** R3
- Mond M, Albrecht D, Kretschmann H M, Heumann E, Huber G, Kuck S, Levchenko V I, Yakimovich V N, Shcherbitsky V G, Kisel V E and Kuleshov N V 2001 *Phys. Status Solidi a* **188** R3
- Podlipensky A V, Shcherbitsky V G, Kuleshov N V, Levchenko V I, Yakimovich V N, Mond M, Heumann E, Huber G, Kreschmann H M and Kuck S 2001 *Appl. Phys. B* **72** 253
- Wagner G J and Carrig T 2001 *OSA Technical Digest on Advanced Solid-State Lasers* (Washington, DC: Optical Society of America) pp 335–7
- Mond M, Albrecht D, Heumann E, Huber G and Kück S 2002 *Opt. Lett.* **27** 1034
- [4] Moskaev I S, Fedorov V V and Mirov S B 2004 *Opt. Express* **12** 4986
- [5] Kasiyan V, Dashevsky Z, Shneck R, Korostelin Y and Landman A 2006 *Optical Materials and Applications; Proc. SPIE* **5946** 594612
Casian V, Dashevsky Z, Shneck R and Rotman S 2003 *Proc. SPIE* **5123** 79
- [6] Vallin J T, Slack G A, Roberts S and Hughes A E 1970 *Phys. Rev. B* **2** 4313
Vallin J T and Watkins G D 1974 *Phys. Rev. B* **9** 2051
Vallin J T and Watkins G D 1972 *Solid State Commun.* **11** 35
- [7] Ryskin A I, Vasil'ev A V, Kremerman V A and Rosenfeld Y B 1992 *J. Lumin.* **52** 83
- [8] Abhvani A S, Bates C A, Clerjaud B and Pooler D R 1982 *J. Phys. C: Solid State Phys.* **15** 1345
Abhvani A S, Bates C A and Pooler D R 1984 *J. Phys. C: Solid State Phys.* **17** 1713
- [9] Bates C A and Stevens K W H 1986 *Rep. Prog. Phys.* **49** 783
Goetz G, Zimmermann H and Schulz H-J 1993 *Z. Phys. B* **91** 429
Martinelli L, Passaro M and Pastori Parravicini G 1989 *Phys. Rev. B* **40** 10443
- [10] Bevilacqua G, Martinelli L and Vogel E E 2002 *Phys. Rev. B* **66** 155338
- [11] Bevilacqua G, Martinelli L, Vogel E E and Mualin O 2004 *Phys. Rev. B* **70** 075206
- [12] Klokishner S I, Tsukerblat B S, Reu O S, Palii A V and Ostrovsky S M 2005 *Opt. Mater.* **27** 1445–50
- [13] Klokishner S I, Tsukerblat B S, Reu O S, Palii A V and Ostrovsky S M 2005 *Chem. Phys.* **316** 83–92
- [14] Malkin B Z 1987 Crystal field and electron–phonon interaction in rare-earth ionic paramagnets *Spectroscopy of Solids Containing Rare-Earth Ions* ed A A Kaplyanskii and R M Macfarlane (Amsterdam: North-Holland) p 13
- [15] Popova M N, Chukalina E P, Malkin B Z and Saikin S K 2000 *Phys. Rev. B* **61** 7421
- [16] Klokishner S, Melsheimer J, Jentoft F S and Schlögl R 2004 *Phys. Chem. Chem. Phys.* **6** 2066
- [17] Clementi E and Roetti C 1974 *At. Data Nucl. Data Tables* **14** 177
- [18] Bersuker I B and Polinger V Z 1983 *Vibronic Interactions in Molecules and Crystals* (Berlin: Springer)
- [19] Perlin Yu E and Tsukerblat B S 1983 Optical bands and polarization dichroism of Jahn–Teller centers *The Dynamical Jahn–Teller Effect in Localized Systems* ed Yu E Perlin and M Wagner (Amsterdam: Elsevier) chapter 7, pp 251–346
- [20] Koster G F, Dimmock J O, Wheeler R G and Statz H 1963 *Properties of the Thirty-Two Point Groups* (Cambridge, MA: MIT Press) p 104